

# Rapid Response Drilling



Past,  
Present,  
and  
Future



# Rapid Response Drilling

Past,  
Present,  
and  
Future

Emily E. Brodsky, Kuo-Fong Ma, Jim Mori, Demian M. Saffer,  
and the participants of the ICDP/SCEC International Workshop  
of Rapid Response Drilling



# Contents

I. Scientific Motivation.....	1
II. How to Solve the Problems: What to Measure and Why.....	3
What Happens Within a Fault During a Big Earthquake?.....	3
How Do Faults Prepare for the Next Earthquake? .....	9
How Do Earthquakes Interact? .....	11
What Are the Important Material and Chemical Properties of the Seismogenic Zone that Control Faulting? .....	12
III. Prior Rapid Fault Zone Drilling Projects.....	13
What Has Been Learned From the Nojima Fault Drilling?.....	13
What Has Been Learned From the Taiwan Chelungpu Fault Drilling Project? .....	14
Wenchuan .....	16
Fault Zone Drilling Projects in the Absence of a Major Earthquake .....	16
IV. Proposed Earthquake Drilling Plan .....	19
Key Observables in a Rapid Response Borehole .....	19
Site Selection Criteria.....	20
Drilling Strategy.....	20
Scenario Drilling and Completion Plan .....	20
V. Recommendations.....	26
Recommendations for ICDP .....	26
Recommendations for the Scientific Community .....	26
Appendix. Workshop Participants .....	27
References.....	28
<b>Boxes</b>	
BOX A. Rubbing Your Hands to Make Them Warm.....	3
BOX B. San Andreas Heat Flow Paradox.....	4
BOX C. The Earthquake Energy Balance .....	7
BOX D. How Deep? How Fast? .....	10
BOX E. Where is the Fault? .....	15
BOX F. Where Will the Earthquakes Happen? .....	21–22
BOX G. Instrument Development Needs for Deep Boreholes .....	25



# I. Scientific Motivation

For millennia, scientists have been asking questions about the physics of earthquakes in the hope that their catastrophic effects can somehow be mitigated. In this past century, significant progress has been made on many issues. We can now generally delineate the regions where earthquakes are likely to occur. We can use seismic waves to measure the size and determine the location of an earthquake. We can model idealized ruptures and predict the resulting ground motions. We can design buildings that are resistant to the shaking near an earthquake. These advances have had direct benefits for the over 100 million people globally who are exposed to earthquake hazards [UNDP, 2004].

However, further progress is largely hampered by a lack of fundamental data about the forces and processes on a fault deep beneath the ground during an earthquake. We do not know how much stress is exerted on the fault during slip and, as a result, can not predict when the stress will break the fault or how far the fault will slip. We do not know how the fault evolves after an earthquake and how its changing structure resumes the strength required to generate more earthquakes. We are mystified by the process that triggers aftershocks even though increased seismicity is one of the most predictable consequences of an earthquake. We struggle to identify what aspects of fault geology are prerequisites for earthquakes and how to identify faults that release stress by simply creeping.

Immediately after a large earthquake, there is an opportunity to gain crucial information to fill these gaps in knowledge. For about two years, the fault is observably changed and a deep borehole can capture measurable signals germane to making progress in earthquake physics. Specifically, a deep borehole can address the following questions:

## What Makes an Earthquake Big? What Happens on the Fault During Large-Slip Events?

Earthquakes occur when the increasing local stress overcomes the frictional strength of a fault. A big earthquake occurs rather than a small one when the strength is pervasively low or the stress accumulation is high over a large region of the fault. Strain accumulation is relatively well understood and monitored through geodesy, however, the strength of faults and their time and slip dependence are much more poorly measured. At large displacements and at high velocities that characterize big earthquakes, even less is known about friction. Current laboratory evidence suggests that

friction could drop dramatically during an earthquake. But how low? No one has measured the friction between two opposing sides of a ruptured fault. Understanding variations in frictional strength and its controlling mechanisms during large earthquakes is key to understanding the faulting process.

## How Do Faults Heal in Preparation for the Next Earthquake?

After a fault slips, local strain is released and the final fault strength may be low due to dynamic frictional processes. In the long intervals between earthquakes, fault strength recovers slowly. Much of this process may not be measurable. However, recent work has shown that there is a window of opportunity after an earthquake when observable proxies for fault strength, such as seismic velocity, ground deformation, permeability, and aftershock rate, all change quickly [Breguier *et al.*, 2008; Kitagawa *et al.*, 2002]. Similarly, laboratory measurements document fault healing due to rate-and-state frictional and physicochemical processes, both of which evolve rapidly following slip [e.g., Hickman *et al.*, 1995; Yasuhara *et al.*, 2005]. The rates of these processes and magnitude of strength recovery is not known and the applicability to the large scale of natural faults is particularly problematic. We need to capture this transient in the field in order to determine the physical processes controlling strength on a fault.

## How Do Earthquakes Interact?

Aftershocks are the most predictable earthquakes. However, the physics of aftershock triggering is still mysterious. Does the dynamic stress of the seismic waves or the static stress change activate the new earthquakes? How does this stress change result in earthquakes that are delayed by weeks or months after the mainshock? Can we predict where and when aftershocks will occur in a precise way?

Current data suggest that up to 80% of earthquakes are generally triggered by another earthquake [Marsan and Lengline, 2008]. Some of these aftershocks themselves are large and damaging. For instance, the M8.7 March 2008 Indonesian earthquake may be considered an aftershock of the M9.2 December 2004 earthquake. Determining the mechanism of triggered events is an important step on the road to earthquake prediction.

## What Are the Important Material and Chemical Properties of the Seismogenic Zone Involved Nucleating Earthquakes?

We are just beginning to understand the physical and chemical properties of active faults from recent fault-drilling projects. Results show that fluids, mineralogy, and deformational structures all play important roles in fault behavior. Specific combinations of these material properties lead faults to episodically slip rapidly as opposed to gradually creep [Dixon and Moore, 2007]. We can only be sure which combinations are necessary by sampling and instrumenting faults that have ruptured in large earthquakes. Furthermore, during healing following an earthquake, new surface area generated by fracturing is attacked by rapid chemical reactions that can destroy the record of slip. Relating geophysical constraints on fault friction and aftershock occurrence to the material properties of the fault zone is essential to a comprehensive understanding of the earthquake process.

These questions drew together 44 scientists representing 10 countries for a three-day workshop on *Rapid Response Drilling: Past, Present, and Future* in Tokyo, Japan, in November 2008. The group discussed the scientific problems and their possible solutions through rapid response drilling. Focused talks presented previous work on drilling after large earthquakes and in fault zones in general, as well as the state of the art of experimental techniques and measurement strategies. Detailed discussion weighed the tradeoffs between rapid drilling and the ability to satisfy a diverse range of scientific objectives. Plausible drilling sites and scenarios were evaluated. This report summarizes the outcome of these discussions in the form of key questions, measurement strategies, and recommendations, with the goal of providing a starting point for drilling after future large earthquakes.

# II. How to Solve the Problems: What to Measure and Why

The scientific questions outlined in Section I require specific measurements, as enumerated below. In order to learn about friction, healing, interaction, and nucleation, measurements of heat, stress, geological structures, frictional properties, permeability, seismic velocity, fluid chemistry, and local ground motion are needed.

## What Happens Within a Fault During a Big Earthquake?

Measuring the frictional resistance to fault slip during an earthquake is critical to building a full physical model of seismic nucleation and rupture. Unfortunately, seismology is not well suited to measuring absolute values of stress because seismic waves are only sensitive to stress changes.

### Temperature Measurements

Temperature is the most direct way to quantify coseismic friction [e.g., *Lachenbruch and Sass, 1980*]. Because most of the frictional resistance is dissipated as heat, any temperature increase on the fault is potentially interpretable as a cumulative measure of frictional heat generation during slip (Box A). To measure the friction of an earthquake, the temperature must be measured in the vicinity of the seismogenic fault as quickly as possible. To obtain the largest and most unambiguous signal possible, it is critical to record these measurements both soon after earthquake slip, and at depths where shear stress (a function of the effective normal stress and the effective coefficient of friction) is sufficiently large to generate an observable temperature anomaly (Figure 1a,b).

In practice, thermal anomalies are detected on the basis of curvature in temperature-depth profiles and departures from a constant background heat flow. However, several processes other than frictional heating can cause deviations from a simple linear geotherm: variations in thermal conductivity with depth, radiogenic heat production, topographic effects, uplift and erosion, or subsidence and burial. Over years, these sources of curvature can be considered steady state and removed by repeatedly logging the borehole and differencing the logs. The effects of thermal conductivity variations can also be defined independently if samples are collected and thermal conductivity measured in the laboratory.

### BOX A. Rubbing Your Hands to Make Them Warm

On a cold day, you may rub your hands together to keep warm. The more pressure on your hands and the longer you rub, the more you warm your hands. Based on the friction of your skin, we can calculate how warm your hands become.



The heat generated in one swipe is

$$Q = \mu \sigma_n \cdot u \cdot S$$

where  $\mu$  is the coefficient of friction,  $\sigma_n$  is the normal stress,  $u$  is distance moved and  $S$  is the surface area. The temperature change in the skin layer is

$$\Delta T = Q / (C \cdot \rho \cdot S \cdot w)$$

where  $\Delta T$  is the temperature change,  $C$  is the specific heat capacity of the skin,  $\rho$  is the density, and  $w$  is the thickness of the skin. Combining the two equations,

$$\Delta T = \mu \sigma_n \cdot u / (C \cdot \rho \cdot w)$$

Skin has a coefficient of friction of 0.4, a specific heat capacity of  $3600 \text{ J kg}^{-1} \text{ K}^{-1}$ , a thickness of about 1 mm, and a density close to water ( $800 \text{ kg m}^{-3}$ ). Most people can press their palms together with a normal stress of about  $3 \times 10^4 \text{ Pa}$ , which is equivalent to 5 kg. So, for a single, 3-cm motion on your hands, the temperature rise is about  $0.12^\circ$ . If you keep rubbing your hands back and forth, you can generate several degrees of warmth!

Now, imagine your hands as the two sides of a fault. This “rubbing” is how friction is thought to generate heat during an earthquake.

Two additional—and unwanted—sources of curvature are transient disturbances to the borehole wall by drilling and fluid flow. Drilling produces a transient disturbance that scales with total drilling time and increases with the use of drilling mud. When drilling ends, the borehole begins to re-equilibrate and the recovery can be characterized through repeated temperature logging. A common rule of thumb is that it takes about four times the drilling time for a borehole to re-equilibrate thermally; in general, the bottom of a borehole re-equilibrates more quickly than the top because the exposure to drilling is shorter. Temperatures within boreholes from previous fault-zone drilling efforts are reported to

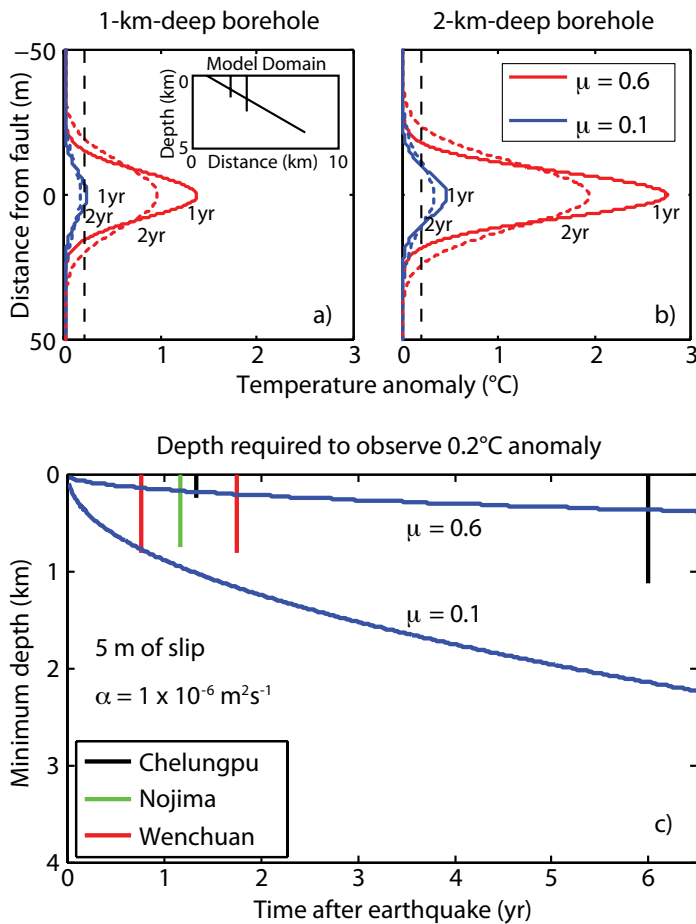


**Figure 1.** Frictional temperature anomalies resulting from a thrust earthquake with 5 m of slip assuming a thermal diffusivity of  $10^{-6} \text{ m}^2\text{s}^{-1}$ . (a) Temperature anomaly for a borehole intersecting the fault at 1-km depth. Red and blue lines show frictional heating for effective friction coefficients of 0.6 and 0.1, representing a strong and weak fault, respectively. Solid and dashed lines show the frictional heating anomaly one and two years after the earthquake, respectively. Dashed black line shows the assumed detection threshold of  $0.2^\circ\text{C}$ . (b) Temperature anomaly for a borehole intersecting the fault at 2-km depth. (c) Blue lines show the minimum depth of borehole intersection with a fault to observe a temperature anomaly of  $0.2^\circ\text{C}$  as a function of time. The depth and timing of borehole completion of fault-zone drilling experiments are shown as vertical lines at the top of the panel [Fulton *et al.*, 2008].

have stabilized to within  $0.01^\circ\text{C}$  within six months after drilling [e.g., Williams *et al.*, 2004; Kano *et al.*, 2006]. Taking these issues into account results in an estimate of the requisite depth for drilling based on the time since the earthquake and the expected value of the coefficient of friction (Figure 1c).

The possibility of advection of frictionally generated heat by fluid flow following an earthquake must also be considered when interpreting downhole temperature data [Kano *et al.*, 2006]. Fulton *et al.* [2008] used a series of two-dimensional numerical models to simulate transient coupled fluid flow and heat transport to illustrate that temperatures across a fault zone should not be markedly affected by fluid flow driven away from the fault by locally elevated pore pressure (e.g., due to thermal pressurization or shear compaction). However, temperatures may be affected after an earthquake by buoyant upflow of warm fluids within a permeable fault zone, or by fluid flow driven by high ambient pore pressures within the surrounding country rock (Figure 2). After a few years, these effects are negligible unless permeability is  $>10^{-14} \text{ m}^2$ ; above this value, significant perturbations to the conductive solution are likely. The perturbations are expected to increase with time as warm fluids migrate from depth. The results of these simulations illustrate that although the shape of a frictional heating anomaly

## BOX B. San Andreas Heat Flow Paradox

It was recognized about 40 years ago that if the frictional strength of faults was as high as indicated by laboratory rock mechanics experiments (coefficient of friction 0.6 to 0.7), there should be an observable heat flow anomaly associated with high slip rate faults, such as the San Andreas. The lack of an observed heat flow anomaly on the San Andreas has been termed the “San Andreas Heat Flow Paradox” [Brune *et al.*, 1969; Lachenbruch and Sass, 1980]. The low heat flow values indicate either (1) the frictional strength of the fault is much lower than laboratory values or (2) there are other factors, such as water flow, that are removing the heat. This issue has been long debated with proponents for both a “high strength” and “low strength” fault. One of the major issues in resolving the paradox is that the existing measurements average dissipation over time and thus do not constrain the transient effects of earthquakes [Zoback and Healy, 1992; Scholz and Saucier, 1993].

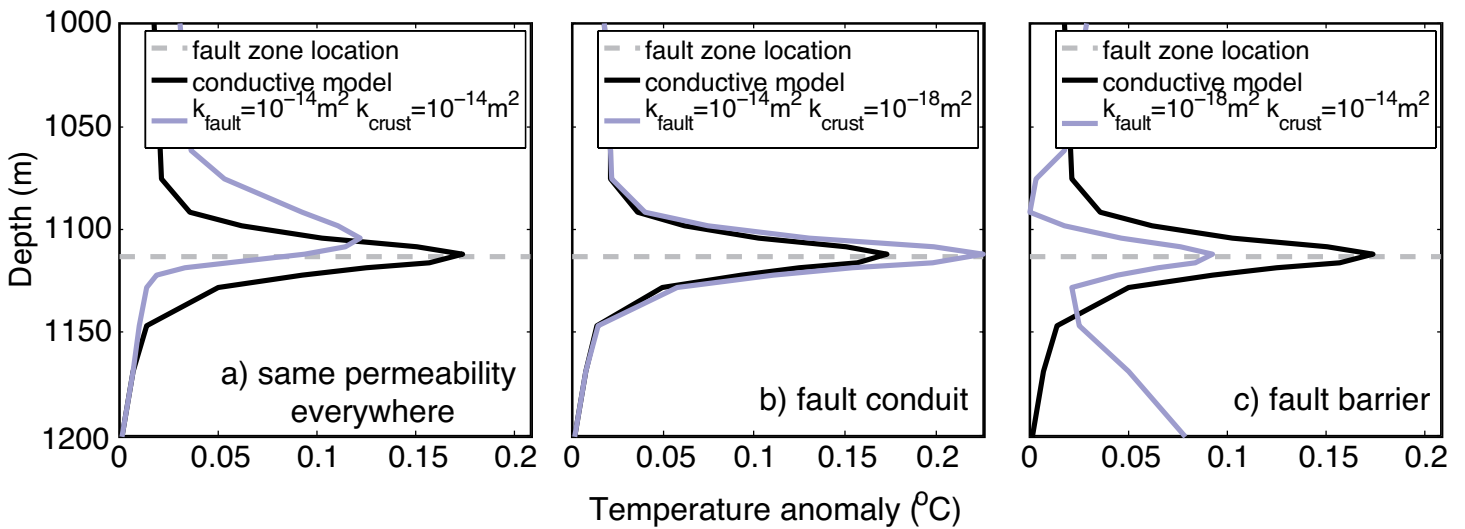


**Figure 2.** Frictional heating anomalies with (blue lines) and without (black lines) significant fluid flow, two years after an earthquake. Conductive anomalies correspond to weak fault scenarios with an effective friction coefficient of 0.07, 5 m of fault slip, and a depth of 1111 m, corresponding to the borehole intersection of the Taiwan Chelungpu Drilling Project. The advective effects of fluid flow are modeled for a high permeability of  $10^{-14} \text{ m}^2$  for (a) the entire model domain, (b) within a 10-m-wide fault zone corresponding to a fault conduit, and (c) only within the country rock surrounding a low-permeability fault zone corresponding to a fault barrier [Fulton et al., 2008].

should be modified somewhat if advective effects are substantial (i.e., in high-permeability cases), it would still be clearly resolvable after two years. Moreover, the use of repeat logs to monitor the evolution of thermal anomalies with time will allow separation of hydrologic (advective) and frictional heating signals.

### Direct Stress Measurements

An alternative approach to quantifying fault strength is to measure absolute stress directly. Stress and earthquakes are known to be interrelated: stress triggers earthquakes and earthquakes alter the stresses on surrounding faults. Determining the stress profile during rapid response fault-zone drilling, including the orientations and magnitudes of three-dimensional stresses, may tell us the stress change induced by fault rupture. This important information improves our understanding of earthquake generation mechanisms and fault rupture propagation.

Unfortunately, there is no foolproof method by which the magnitudes and orientations of three-dimensional stresses can be reliably measured at great depths, although various field and laboratory measurement techniques have been proposed. For scientific deep-drilling projects, the combined application of borehole methods and core-based methods is necessary to obtain a complete, three-dimensional picture of stress and to enhance the reliability of the stress measurement results (Figure 3). First, a basic borehole data

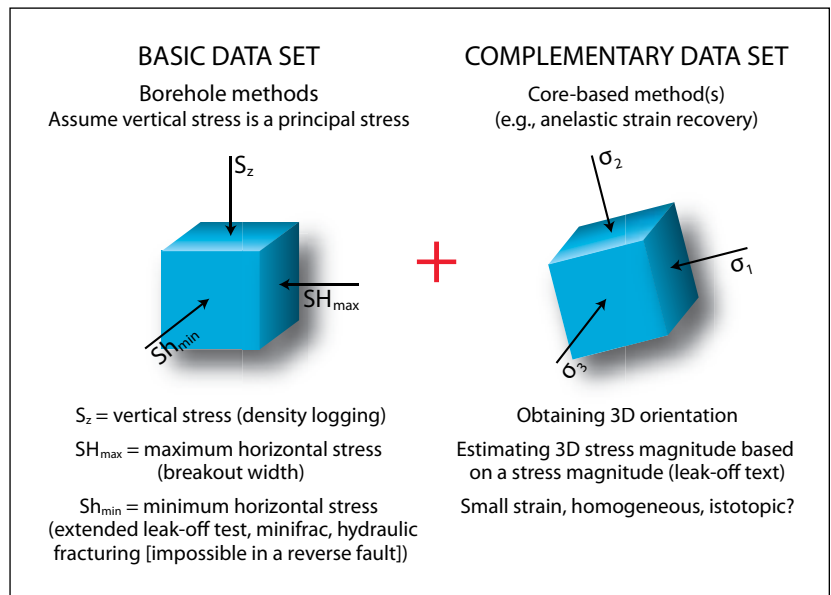


**Figure 3.** A strategy for obtaining reliable stress measurement in deep-drilling wells includes combining borehole and core-based data.

set should be obtained based on an assumption that the vertical stress is one of three principal stresses. The following quantities must be measured: the vertical stress by downhole density logging, minimum horizontal stress by extended leak-off test/minifrac/hydraulic fracturing, and maximum horizontal stress by breakout width analyses [Zoback et al., 2003].

However, it is possible that breakouts will not be observed because of the local stress conditions, strength of the borehole wall, and borehole mud weight. In addition, the hydraulic fractures occur in a horizontal plane in reverse fault stress regimes because the vertical stress is the minimum stress. As a result, the minimum horizontal stress magnitude cannot be determined. Furthermore, hydrofracture is inherently an invasive process that changes the permeability structure in the nearfield of the target fault zone. Hydrofracture experiments are best suited for determining the absolute stress a long time after the tectonic stress field has re-equilibrated.

A good complement to borehole data is core-based data. Anelastic strain recovery (ASR) tests (Figure 4), for example, should be attempted to produce complementary stress data [Lin et al., 2006]. ASR is a three-dimensional method that doesn't assume that the vertical stress is a principal stress. This assumption is suitable for great depths where the anelastic strain is relatively high. Unfortunately, core recovered near the primary slip zone is often highly fractured or composed of soft gouge. Strain is difficult to measure in this type of material through ASR tests, so ASR work should be focused on the outer edge of the damage zone. ASR will only capture transient stresses if the measurement is made immediately after the earthquake. The longer the drilling is delayed, the more the stress will have decayed.

## Geology of Cores and Boreholes

Some of the clearest evidence for the faulting process and frictional dissipation is preserved in fine-scale structures in the core. For instance, the presence of any melt rock (pseudotachylyte) is



**Figure 4.** Anelastic strain recovery measurement of absolute stress on a core sample.

an immediate indicator of high friction early in the slip process as heat is required to melt the rocks. Depending on the melt composition and permeability of the host, low friction during slip may be inferred later in the earthquake once melt has lubricated the surface. Geometric structures can also be used to assess the dynamic fluidization of the gouge and thus likely rheology [Rowe et al., 2005; Brodsky et al., 2009; Boullier et al., in press]. If pseudotachylyte or fluidization structures are found, follow-up laboratory experiments are critical to determining the rheology of the melt or granular flow.

As an example, Figure 5 shows a foliated gouge and isotropic, gouge-bearing, agglomerated, snowball-like structures that have been produced during high-speed laboratory experiments [Boutareaud et al., 2008]. Individual grains have accumulated a ring of very fine-grained, oriented clays during high-speed slip. In these experiments, the round particles behaved like ball bearings and thus reduced the friction. Similar structures have been described in the Chi-Chi principal slip zone [Boullier et al., in press].

Grain-size distribution also contains key information about dissipation. The energy that is absorbed in fracturing and surface creation is energy that is not dissipated by any other means, like friction (see Box C).

Similarly, measurements of fracture density in the borehole wall taken using borehole imaging tools such as the Formation Micro Imager (FMI) and Resistivity-at-Bit (RAB), and in the core itself, constrain the dissipated energy, including that expended off the primary slip surface. Thus, observing the structure in a natural core provides some insight into frictional behavior. Borehole imaging also provides information on the geometry and nature of structures interpretable in terms of long-term strain.

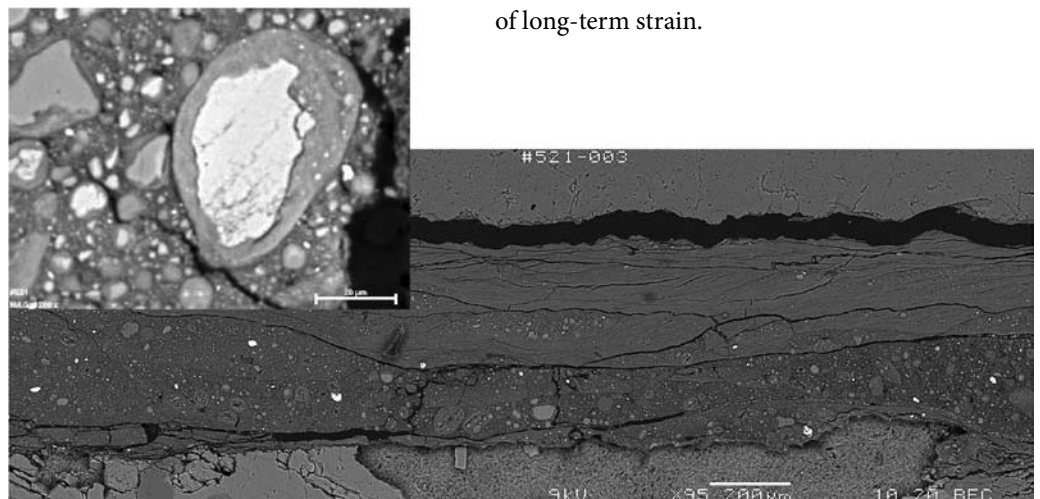


**Figure 5.** Fine structure of fault rock generated during laboratory experiments. Foliated (above) and isotropic (below) gouges are on the left and clay clast aggregates are on the right [Boutareaud et al., 2008].

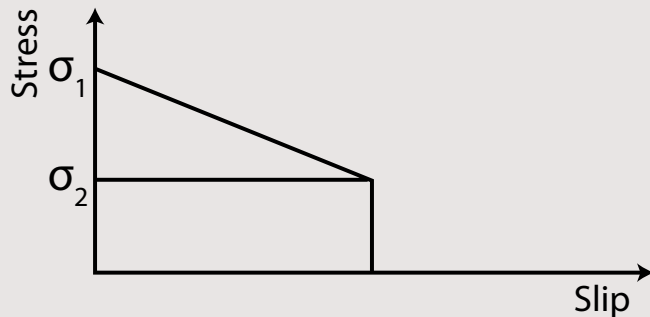
## BOX C. The Earthquake Energy Balance

An earthquake converts elastic strain energy into kinetic energy that is radiated in the form of seismic waves. Predicting the radiated energy and ensuing ground motion is one of the fundamental jobs of seismology. However, only a fraction of the elastic energy is released in seismic waves. The rest is dissipated through some currently unknown combination of friction, surface generation, and chemical processes. Here, we outline the constraints on that energy budget and a method for connecting the geological and seismological data.

For an earthquake that begins with an average stress of  $\sigma_1$  on a fault and ends with an average stress of  $\sigma_2$ , the total elastic energy available is  $\Delta W = (\sigma_1 + \sigma_2)/2 Ad$ , where  $A$  is the area of the rupture and  $d$  is the average slip (see area of schematic diagram). The resulting energy balance is

$$\Delta W = E_f + E_R + E_G \quad (\text{C.1})$$

where  $E_f$  is the frictional energy,  $E_R$  is the radiated energy and  $E_G$  is the fracture energy [e.g., *Kanamori and Brodsky, 2004*]. In this formulation, all nonfrictional dissipative processes



Fault-zone mineralogy changes rapidly during the healing process. Geophysical indicators discussed below suggest that the healing process progresses dramatically over a few months. Clays break down and veins fill with precipitates. To get the best view of the earthquake, one must observe the core as quickly as possible.

### Laboratory Measurements

Most prior work on fault friction has been based on laboratory experiments on rocks sliding with limited velocities. One of the problems with real earthquakes is that the unusual mineralogy,

are lumped together in  $E_G$ . To conveniently relate the energy balance to observable seismological quantities, a further separation is made between the slip-dependent component of friction,  $E_{f\_vary}$  and the constant component. By definition, the constant component of the frictional stress is  $\sigma_2$ . So, the constant component of the frictional energy is  $\sigma_2 Ad$ .

Rearranging the energy balance using this separation and substituting for  $\Delta W$  in terms of  $\sigma_1$  and  $\sigma_2$  results in

$$(\sigma_1 - \sigma_2)/2 Ad = E_{f\_vary} + E_G + E_R \quad (\text{C.2})$$

Because the seismic moment  $M_0$  is easily measurable using modern seismic methods and  $M_0 = \mu_s Ad$  where  $\mu_s$  is the shear modulus, a more convenient form of the equation is

$$E_{f\_vary} + E_G = \Delta\sigma M_0 / 2\mu_s - E_R \quad (\text{C.3})$$

where  $\Delta\sigma$  is the static stress drop  $\sigma_1 - \sigma_2$ . This required overall energy balance of an earthquake can be used as a tool for connecting the various observables and combining their constraints on the micromechanics of rupture. All of the terms of the right-hand side of eq. C.3 are observable from seismology. Those on the left can only be determined from studies of the geological material of the fault. As we search for a complete description of the micromechanics of dissipation, we can evaluate whether or not all processes are accounted for by adding the energy used in each process and comparing it to the energy budget of eq. C.3. Once all processes are identified, eq. C.3 must be in perfect balance.

grain distribution, hydrological conditions, and structure in the fault zone may significantly complicate the local frictional properties. Laboratory experiments can be manipulated to ascertain the exact effective stress and slip conditions to generate the observed stresses from the available materials. Furthermore, direct measurements of friction in the lab help to assess the applicability of the great body of rock mechanics to actual earthquake fault conditions.

To diagnose the relative importance of various physical mechanisms during the earthquake, the frictional properties of gouge from the center of the fault zone (its core) need to be measured in a laboratory and the results compared to the stresses inferred from the temperature and core-based stress measurements. Recent large velocity experiments on natural gouge removed from faults' cores show that significant weakening occurs as slip progresses (Figure 6). Still, these final friction values are somewhat higher than inferred from the temperature in the same locales [Tanaka *et al.*, 2006; Kano *et al.*, 2006]. If such low frictional coefficients are reproduced in a more rapid measurement, the fault gouge must be manipulated in the lab to reproduce the effect. Possible candidate

processes that could be reproduced include elastohydrodynamic lubrication at high speeds and thermal pressurization with large water fractions [Brodsky and Kanamori, 2001; Andrews, 2002].

Laboratory measurements do not need to be made immediately, but are a necessary complement to measurements of the transient stress discussed earlier.

## Hydrogeology

A number of hypothesized dynamic fault weakening mechanisms rely critically on the transient development of elevated pore fluid pressure via thermal or poro-elastic processes; the total effect of these transient mechanisms also depends on the initial (ambient) pore fluid pressure. In order to assess the sealing potential of the fault, permeability must be measured. Permeability measurements in a fault zone are also an important contribution in their own right. The extent to which fluids may be trapped in a fault zone determines both the shear stress during an earthquake and the locking strength before the next one. In addition, permeability is a measure of damage, because permeability in the damaged zone adjacent to the fault is usually dominated by fractures.

Cross-hole injection or pumping experiments provide the most direct measurement of effective permeability at the formation scale. Borehole permeameters can be used to obtain a small-scale, near-borehole profile, but are generally limited to permeabilities greater than  $\sim 10^{-16} \text{ m}^2$  due to the longer equilibration times required in low-permeability formations. Laboratory measurements of core samples were successful for both the Nojima and Chelungpu fault-zone drilling projects, although these measurements can only assess centimeter-scale hydrological structure. As will be discussed, alternative techniques exist to measure time-dependent permeability.

Direct measurements of pore pressure are also important for evaluating static friction, because elevated pore pressure reduces the effective normal stress on faults and their overall shear strength [e.g., Hubbert and Rubey, 1959; Rice, 1992]. Although direct pore pressure measurements have not been made within the San Andreas Fault Observatory at Depth (SAFOD), preliminary interpretations based on drilling observations suggest that the fault zone is not overpressured at the depth where it is intersected by the borehole [Zoback and Hickman, 2005]. Similarly, in situ pore pressures on the Chelungpu Fault are inferred to be low enough as to be inconsistent with a static, long-term elevated pore pressure trapped within the fault [Doan *et al.*, 2006]. These observa-

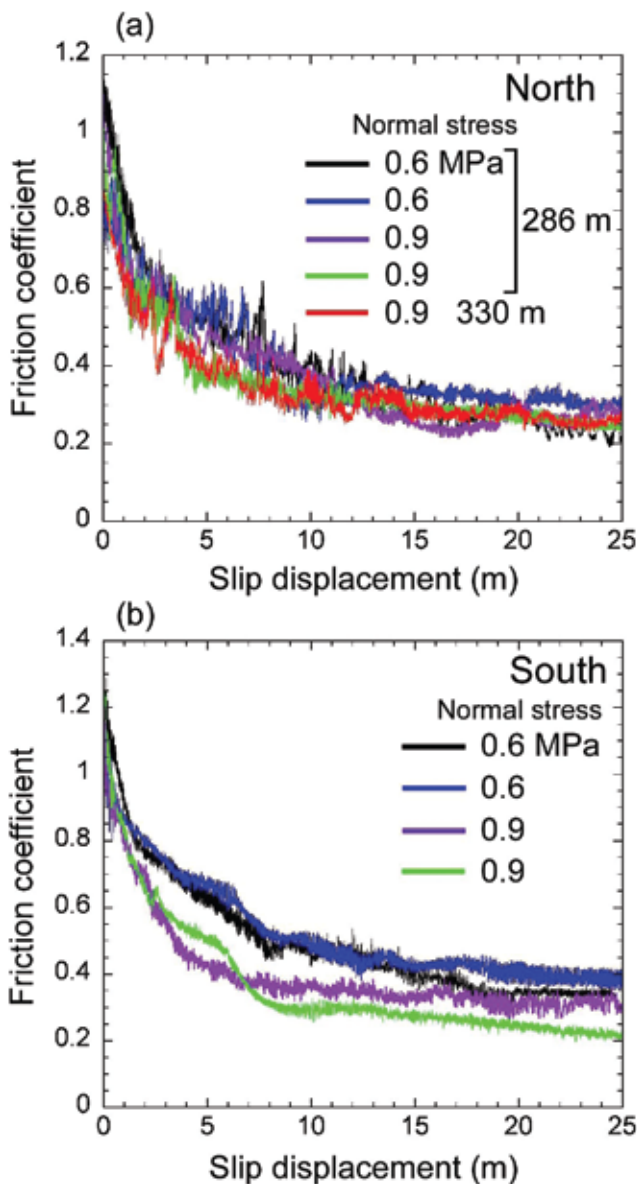


**Figure 6.** Tanikawa and Shimamoto [2009] experiments on fault gouge, which show that significant weakening occurs on a fault as slip progresses.

tions suggest that long-term weakening from high pore pressure may not be an adequate explanation for the apparent weakness of these fault zones.

In summary, solving friction questions requires using a variety of techniques, all of which benefit from a deep borehole drilled within a short period after an earthquake. The results must be combined with modeling studies for physical interpretation. The most synergistic studies have incorporated modeling work as early as possible into the observational studies in order to motivate new observations while the research is still in progress.

## How Do Faults Prepare for the Next Earthquake?

Fault-healing observations are essential for understanding the recovery mechanisms of faults. Healing processes have recently been captured by taking measurements of seismic velocity changes and hydrological properties in the months to years following earthquakes. Healing signatures might also be observable in other types of geophysical logs. Because aftershock rates and other observed transients decay as  $1/\text{time}$ , measurement campaigns will be most effective if they are begun quickly. Although all of these proxies for fault evolution have been used in isolation, they have never been combined on a single fault.

### Seismic Velocity

Seismic velocity has been shown to increase on a fault immediately after an earthquake (Figure 7) [Li *et al.*, 1998; Li and Vidale, 2001; Vidale and Li, 2003]. Most spectacularly, a recent noise cross-correlation study showed velocity changes following the 2004 Parkfield earthquake that correlate with the slowly decaying strain transient (Figure 8). Changes in scattering and attenuation have also been reported in connection with stressing faults [Niu *et al.*, 2003, 2008]. However, it is unclear if the seismic velocity change is an entirely shallow phenomenon or records a deeper process that is

fundamental to the rheology of the fault; thus, measurements in a deep borehole are essential. Because changes often decay as  $1/\text{time}$ , measurements soon after an earthquake are important (see Box D for a more detailed discussion on depth and time considerations). Repeated vertical seismic profiles (VSPs) to measure velocity at depth in the nearfield of the fault could capture the progression of fault healing and changes in elastic moduli in the critical time period of the strong aftershock sequence. Borehole measurements should be complemented with short-term surface deployments of short-period seismometers as soon as possible after the earthquake, with repeat deployments continuing at one- to two-year intervals after the earthquake.

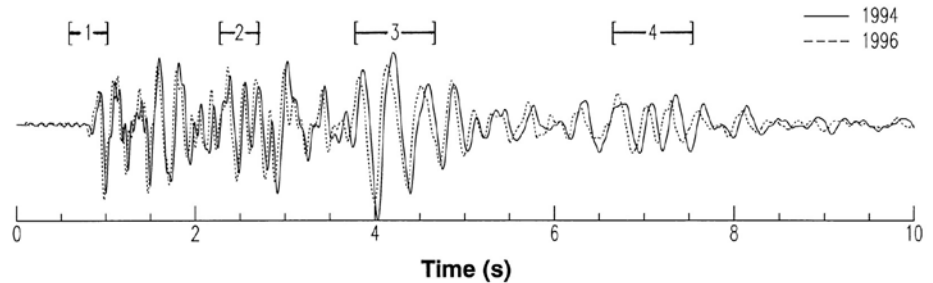


**Figure 7.** Seismograms showing increasing seismic velocity in the Landers, CA, fault zone following the earthquake. The earthquake occurred in 1992. Seismograms are from active-source experiments in the fault zone done in 1994 and 1996. Note the earlier arrivals late in the wavetrain in 1996. The increasing velocity is interpreted as restrengthening of the fault, but the depth of the structural change is poorly constrained [Li *et al.*, 1998].

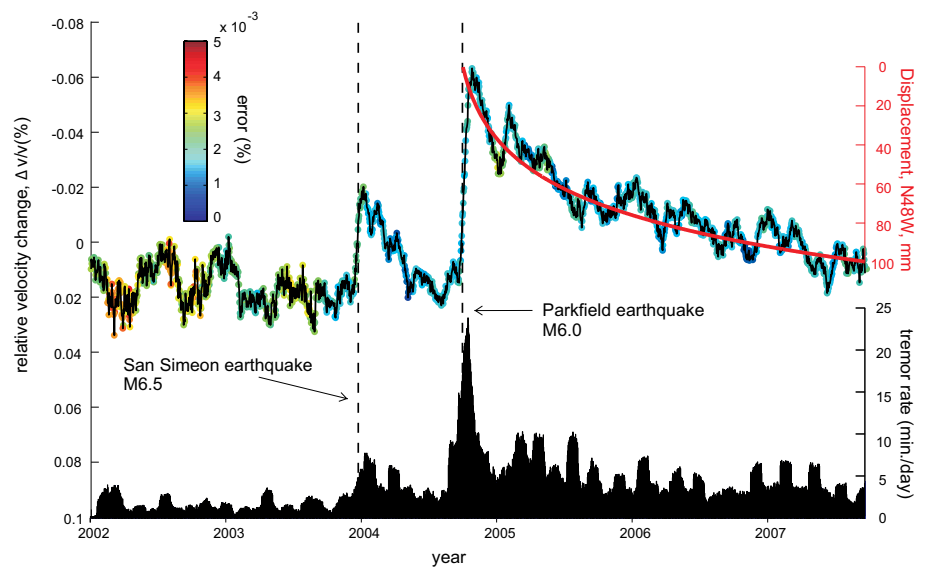


**Figure 8.** Seismic velocity decay measured from the cross correlation of ambient noise measured at Parkfield, CA, in a shallow borehole array [from Brenguier *et al.*, 2008]. The velocity healing signal tracks the displacement measured by GPS (red curve) and the tremor generated deeply on the fault (black bottom curve).

## BOX D. How Deep? How Fast?

One of the first questions confronting any rapid response drilling project is the depth and speed at which it is meaningful to drill. Sometimes a shallow hole can be completed quickly and a deep hole takes more planning and time to arrange funding. Therefore, it is important to ask what the minimum depth and maximum time at which meaningful data can be collected. The answer depends on which questions a project aims to address.

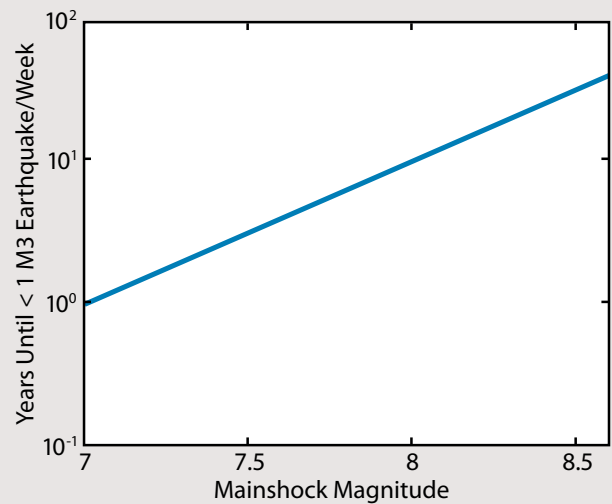
If a drilling project is meant to address **fault friction**, Figure 1c provides a clear estimate of the tradeoff between depth and speed. Because dynamic friction coefficients as low as 0.2 have been observed in the laboratory and 0.1 has been suggested from previous drilling work, a hole that is fully completed two years after the earthquake must reach at least 1.5-km depth.

Questions of **fault zone healing** are limited by Omori's law. At Parkfield, seismic velocity remains measurably depressed for about two years (Figure 8). Local geology determines the appropriate depth for healing questions. It is important that the hole extend below the sedimentary cover as the critical questions of healing revolve around separating the signature of velocity changes in the soil as opposed to the underlying hard-rock.

To address the question of **earthquake interaction**, it is important to drill while seismicity is still substantial. Because such a deployment should easily capture  $M=1$  earthquakes, a level of at least one M3 earthquake per week should be sufficient. We can calculate the speed required for typical aftershock productivities by combining Omori's Law and Gutenberg-Richter with typically observed parameters resulting in

$$N_{\text{aft}} = C 10^{-bM} 10^{\alpha M_m / t^p} \quad (\text{eq. D.1})$$

where  $N_{\text{aft}}$  is the number of aftershocks of magnitude  $M$  or greater,  $M_m$  is the magnitude of the mainshock,  $t$  is time and  $C$ ,  $b$ ,  $\alpha$ ,  $p$  are empirical constants (see figure). For instance, for a M7 earthquake, aftershock sequences typically decay to about one M3 earthquake per day at about one year, so the drilling project must be completed very quickly. For earthquake interaction questions, the hole should be instrumented before this point. Larger earthquakes provide a longer window of opportunity after the mainshock. Depth is not critical for



Time to decay to a low seismicity level for typical seismicity statistics using eq. D.1. Here it is assumed that  $C = 0.005$  earthquakes/day and  $\alpha = b = p = 1$ .

this problem. The hole must simply be deep enough that seismic waves are relatively unattenuated by shallow sediments. Of course, the deeper and closer to the earthquake source, the better.

For questions of the **material properties required for seismogenesis**, the hole should extend into the nucleation zone. Ideally, this depth will be constrained by the depth of initiation of the mainshock. In exceptional geological settings, like that explored by SAFOD, earthquakes nucleate and initiate at 2–3-km depth. Therefore, 2–3 km is a minimum depth for investigating nucleation problems. The geological conditions for propagation are more general, however, the near-surface layers, especially in sediments, do not have the shear strength to accumulate large amounts of strain energy. During large earthquakes, the motion of these shallow portions are likely just “going along for the ride” due to motions from deeper portions of the fault. Furthermore, observations that there are usually few shallow aftershocks less than 1-km deep is another indication that the near surface is not seismogenic. The timing of a drillhole is not critical for determining the materials properties of the seismogenic zone. The timing issues are identical to the fault zone healing ones in that the chemical reactions that proceed on the time scale of healing may erase the evidence of the pre-earthquake geology and chemistry.

## Permeability

Hydraulic diffusivity is a key parameter in models of dynamic weakening because leakage of water out of the fault releases pressure (and hence re-elevates friction). Thus, assessing the effective stress at seismic conditions requires knowledge of the fault's permeability structure. Furthermore, permeability is very sensitive to interconnected fractures and thus is a good measure of the fault's stiffness, which affects post-seismic stress evolution.

Permeability is known to evolve quickly after an earthquake rupture [Kitagawa *et al.*, 2002]. Open fractures fill with precipitates and the fault heals [Geraud *et al.*, 2006; Hiramatsu *et al.*, 2005; Tenthorey *et al.*, 2003]. An accurate assessment of relevant properties, such as hydraulic diffusivity, during and following the earthquake requires a measurement of the permeability shortly after an event (days to months) and then repeated measurements to track its evolution. Permeability changes also likely record fault healing, which may be a key component of the earthquake cycle.

Techniques for continuous monitoring of permeability involve either repeated injections or drawdowns [Kitagawa *et al.*, 2002] or passive monitoring of the natural forcing of Earth tides (Figure 9) [Elkhoury *et al.*, 2006]. Both could be implemented through appropriate completion of the borehole. The field measurements should be complemented by core-scale permeability measurements.

## Fluid Chemistry

Healing is, in large part, a chemical problem. Precipitates close fractures and generate adhesion. Therefore, the fluid chemistry must be sampled to develop a physical-chemical model of the

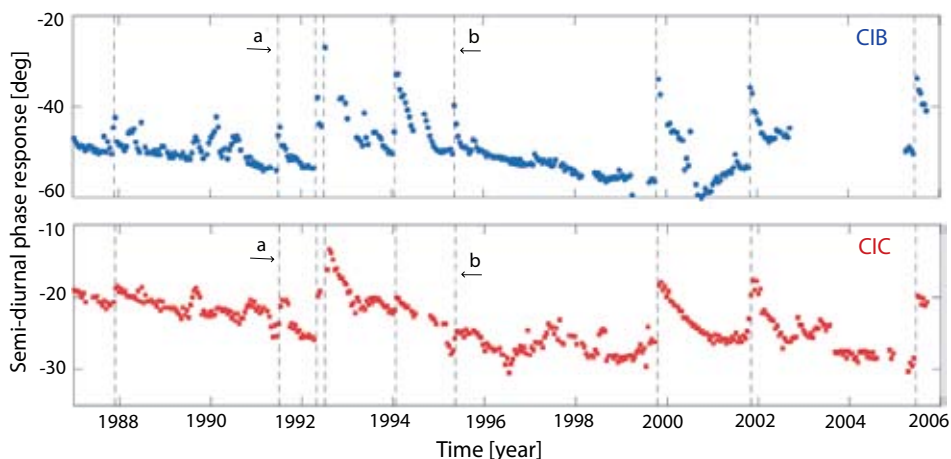


**Figure 9.** Phase lag of the response to solid Earth tides in two shallow water wells. Phase lag is a proxy for permeability, which can be continuously measured to provide a method of recording permeability change. Dashed lines indicate regional earthquakes. Seismic waves from these earthquakes caused permeability changes in the wells that were effectively measured by the phase-lag method [Elkhoury *et al.*, 2006].

healing process. Repeated samples of the formation fluid should be taken throughout the healing process, preferably from the fault core region (highly brecciated zone within the fault) as well as the damage zone.

## How Do Earthquakes Interact?

Aftershocks provide an excellent opportunity to study earthquake interaction, and the most progress will be made if the earthquakes can be studied at close range. Current work on earthquake triggering suggests that the smallest earthquakes are crucial to determining the course of the ensuing sequence. Earthquake sequences seem to be cascades in which one earthquake triggers another, which triggers another [Felzer *et al.*, 2004; Helmstetter *et al.*, 2005]. In these models, the size of the triggered earthquakes can be larger than the earthquake that triggered them as long as the full earthquake population follows the usual size distribution (Gutenberg-Richter law). Because very small earthquakes are extremely abundant and are constantly generating their own aftershocks, the smallest earthquakes therefore play a pivotal role in triggering the larger ones. In the most extreme proposals, the earth is continually being shaken and retriggered by unobservably small earthquakes. There should also be a minimum size of earthquakes and this minimum size will govern the overall probability of generating more earthquakes [Sornette and Werner, 2005]. Yet, this minimum size remains elusive.

Very small earthquakes are best studied from a deep borehole. Earthquakes of magnitude -3 can be routinely observed in a borehole and even smaller ones can be captured if the seismicity level is high enough. Validating or refuting the cascade models requires measuring the relative timing and location of the extended earthquake sequences so that the relationship between the earthquakes can be mapped out. Do very small earthquakes continue to follow the statistics of larger sequences or is there a lower cutoff at which some other physics becomes dominant? What is the stress field generated around each earthquake and how does that stress affect the ensuing sequence? Downhole seismometers, strainmeters, and tiltmeters could provide such data by measuring the displacement on the main fault during aftershocks and thus directly constraining

the mode of earthquake interactions. The instruments will also provide location and timing data on the smallest earthquakes that glue together the aftershock sequence.

## What Are the Important Material and Chemical Properties of the Seismogenic Zone that Control Faulting?

The recovered core can immediately answer this question. Will the fault be filled with phyllosilicates as was found on the creeping section of the San Andreas or is the fault mineralogy substantially different on faults that generate large earthquakes? Mineralogical identification on the bulk sample, in thin section and with analytical tools in the laboratory, can make a major contribution to earthquake science very quickly. Real-time gas and hydrological monitoring will be critical for ascertaining the in situ chemical conditions.

Once the mineralogy and fluid state of the core material is determined, the stage is set to test its frictional properties in the laboratory. If the material is from the seismogenic zone, it must be velocity weakening. Therefore, a key experiment is to determine the conditions under which it is velocity weakening in the laboratory. How much fluid is required? What other chemical conditions are required? Once these conditions have been determined, their stability over time in a geological fault zone can be evaluated. This information can then be combined with the information gained on fault zone healing to evaluate the duration of the preparatory process of an earthquake.

# III. Prior Rapid Fault Zone Drilling Projects

Rapid drilling into a fault zone after an earthquake has already been done in the Nojima Fault, Japan, and the Chelungpu Fault, Taiwan. These pioneering projects have exposed both the challenges and potential benefits of rapid response drilling. Future projects will build on this knowledge base. For reference purposes, we summarize their accomplishments below. We also discuss the knowledge base built by fault zone drilling projects executed in the absence of a large earthquake.

## What Has Been Learned From the Nojima Fault Drilling?

Following the 1995 Kobe earthquake (Mw6.9), the first rapid fault-drilling project was carried out on the Nojima Fault, which had surface rupture of about 1–2 m. The Geological Survey of Japan, National Institute for Earth Science and Disaster Prevention, and a group of Japanese universities drilled seven boreholes to depths of 500–1800 m. The boreholes were quickly completed in 14 months following the earthquake and provided the opportunity for international collaborative studies on the general knowledge on faulting and related seismic processes.

Extensive geophysical measurements were made using standard logging techniques, along with borehole televiewer (BHTV), fullbore formation microimager (FMI), and dipole shear sonic imager (DSI) recordings. Resistivity, seismic velocity, and the various imaging techniques were useful for identifying fault zones and other physical properties throughout the drilled section. The borehole logging results were also correlated with the geological features of the core, such as fault gouge and cataclasites [Ikeda, 2001a]. Temperature measurements with relatively low resolution were made with the standard logging tools, but no signal associated with frictional heating was seen in the vicinity of the fault.

The boreholes provided nearly continuous core samples through the fault within granitic rocks and have shown that geology of the Nojima Fault is more complex than initially thought. The fault zone and principal slip zone thicknesses increase with depth and result from two distinct periods of seismic activity accompanied by intense hydrothermal alteration separated by a quiescence stage, all of the

three of which are transcribed into the microstructures [Ohtani *et al.*, 2000; Boullier *et al.*, 2004a; Tanaka *et al.*, 2007]. The first period (<40 Ma) is characterized by ultracataclasites and pseudo tachylytes formed at 10-km depth or more and are related to M6 to M7 past earthquakes around 56 Ma, and by zeolites as the principal alteration minerals [Boullier *et al.*, 2001; Murakami and Tagami, 2004]. Siderite characterizes the quiescence stage (< 40 Ma, > 1.2 Ma). The second period of seismic activity (< 1.2 Ma) is characterized by thin gouge zones and by carbonates as the principal alteration minerals. The composition of the carbonate veins formed by co-seismic fluid distribution is consistent with fluid circulating presently through the fault [Boullier *et al.*, 2004b; Fujimoto *et al.*, 2007]. Textural and geochemical investigations have provided spatial distribution of deformation and alteration intensity, and mass transfer in the fault zone with volume loss in the main shear zones and volume gain in the damaged zone [Tanaka *et al.*, 2001, 2007]. Healing by mechanical compaction and by dissolution-diffusion-deposition mechanisms may be very efficient, making it difficult to recognize the principal slip zone in the Geological Survey of Japan borehole one year after the earthquake. This drilling project renewed international interest in pseudotachylytes, high-speed friction experiments on hard rocks and the thermal budget of earthquakes..

Repeated water-injection experiments are being done in the 1800-m borehole to look for changes in fault permeability. Starting one year after the earthquake, and at subsequent intervals of a few years, water is pumped into the region of the fault to induce small earthquakes. The timing and location of induced earthquakes, along with monitoring of resistivity, indicated permeabilities of  $10^{-16}$ – $10^{-14}$  m<sup>2</sup> two years after the earthquake [Tadokoro, 2001; Murakami *et al.*, 2001]. Subsequent injections suggest at least a 50% decrease in permeability over the subsequent three years [Kitagawa *et al.*, 2002].

Estimates of the orientation of the local stress field were done with hydrofracturing in boreholes and stress measurements on cores [Ikeda *et al.*, 2001b, Tsukahara *et al.*, 2001; Yamamoto and Yabe, 2001]. All three studies showed directions of maximum compressive stress at high angles that are nearly perpendicular to the fault, indicating low values for the static coefficient of friction.

## What Has Been Learned From the Taiwan Chelungpu Fault Drilling Project?

An outstanding feature of the 1999 Chi-Chi, Taiwan earthquake (Mw 7.6) was the extended surface rupture of the out-of-sequence thrust fault. The fault break was clearly visible for about 100 km, with surface displacements of 1–12 m in between layers of sandstone and shale. The distribution of shallow slip on the fault allowed access to an area of large slip with drilling. The Taiwan Chelungpu Fault Drilling Project (TCDP) drilled two boreholes 40 m apart that penetrated the dipping thrust fault at depths of about 1110 and 1130 m. The nearby surface fault had a displacement of about 12 m. The boreholes were completed 65 and 73 months after the earthquake. There were also two shallow boreholes to depths of 330 and 180 m on the northern and southern portions of the fault, respectively. These shallow boreholes were completed 18 months after the earthquake [Tanaka *et al.*, 2006].

Temperature measurements were made in both the shallow and deep boreholes located in the northern region of large slip [Tanaka *et al.*, 2006; Kano *et al.*, 2006]. Both studies found a consistent low level of residual heat close to the fault. In terms of frictional levels, these measurements infer a very low apparent coefficient of friction around 0.1 to 0.2 (Figure 10). Issues of water flow and determination of thermal diffusivity complicate the interpretation, however, these results show the potential importance of the temperature measurements at depth following a large earthquake.

The earthquake is distinguished by different seismological signatures in the northern and southern parts of the Chelungpu fault in terms of total slip and high-frequency energy [Ma *et al.*, 2001; Chen *et al.*, 2001]. These distinctions are associated with different microstructural signatures and permeability properties as shown by samples from the two shallow boreholes [Tanikawa and Shimamoto, 2009]. Pseudotachylytes reworked in several

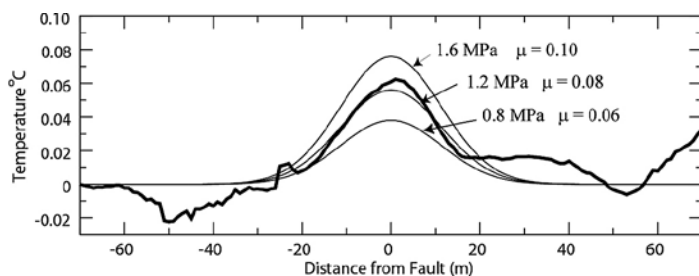


**Figure 10.** Temperature anomaly recorded in the Taiwan borehole and interpretation in terms of maximum friction coefficient [Kano *et al.*, 2006].

seismic events have been described in the south (higher friction) when several clayey injections were observed in the north [Otsuki *et al.*, 2005].

The TCDP site was chosen near Dakeng in the northern part of the fault where the earthquake had particularly large slip and slip velocities in order to investigate the energy budget and the slip-weakening mechanisms of the Chi-Chi earthquake [Ma *et al.*, 2003]. Identification of the fault zone required combining multiple techniques (See Box E). The data together indicate a slip zone at 1111 m in Hole A (FZA1111) and 1136 m in Hole B (FZB1136) situated at 39 m down dip, apart from Hole A [Kuo *et al.*, 2005; Ma *et al.*, 2006; Yeh *et al.*, 2007; Hung *et al.*, 2007; Sone *et al.*, 2007; Hirono *et al.*, 2008]. Evidence that the black gouges in these regions are in fact the slip surface includes clay mineralogy, isotropic texture, absence of later reworking microstructures, and a very fine grain size indicative of high fracture energy in the Chi-Chi earthquake's energy budget [Ma *et al.*, 2006].

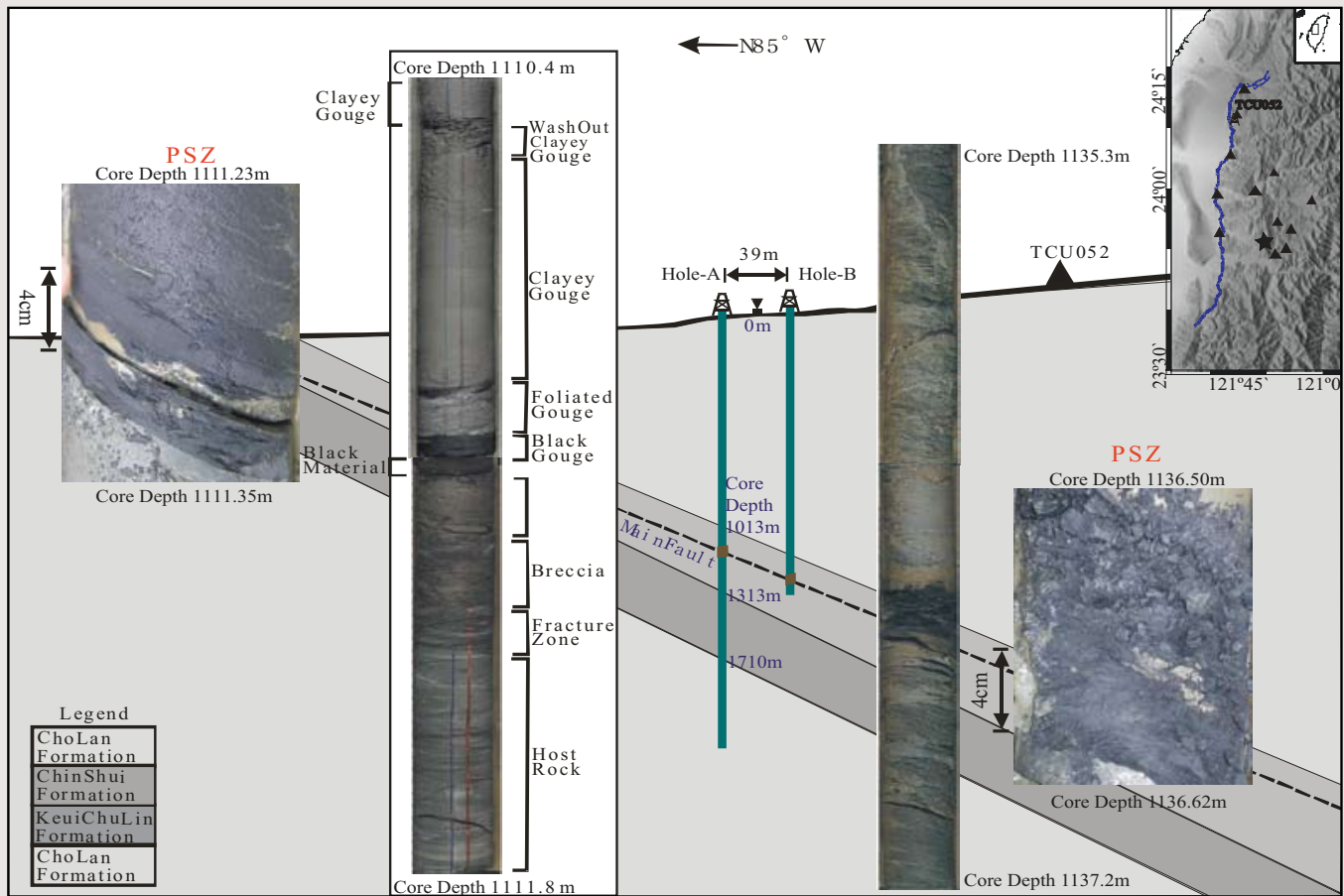
Physical properties have been measured continuously on cores from Hole B using nondestructive methods [Hirono *et al.*, 2007a]. Clay-clast aggregates similar to those experimentally reproduced during high-velocity rotary shear experiments and inverse grain size segregation (Brazil Nut Effect) were found in the FZA1111 principal slip zone and were interpreted as evidence for gouge fluidization as a result of frictional heating and thermal pressurization [Boutareaud *et al.*, 2008; Boullier *et al.*, in press]. In FZB1136, the Chi-Chi principal slip zone is a 3-mm-thick layer of foliated gouge [Boullier *et al.*, in press]. Several other pieces of evidence, such as a magnetic susceptibility anomaly [Hirono *et al.*, 2006; Mishima *et al.*, 2006], clay mineralogy [Kuo *et al.*, 2005; Hashimoto *et al.*, 2008], whole-rock chemistry [Ishikawa *et al.*, 2008; Hirono *et al.*, 2007b], and gouge injections [Otsuki *et al.*, 2005; Boullier *et al.*, in press], show that the principal slip zone related to the Chi-Chi earthquake, as well as principal slip zones related to similar past earthquakes, have been heated to as much as 900°C and, consequently, are thermally pressurized and fluidized [Hirono *et al.*, 2007b]. Fluid circulation seems to be limited in the Chelungpu Fault, but healing processes and aseismic deformation by dissolution-diffusion-deposition mechanisms are important and efficient processes in the fault and damage zones [Boullier *et al.*, in press].

A cross-hole pumping test indicated a permeability of  $10^{-18}$  to  $10^{-16}$  m<sup>2</sup> along the fault and simultaneous monitoring data suggested that the fault zone is moderately overpressured [Doan *et al.*, 2006]. Laboratory results on the shallow core samples show that the permeability of the northern region is an order of magnitude less than for the southern region [Tanikawa and Shimamoto, 2009].

## BOX E. Where is the Fault?

One of the most challenging aspects of recent fault zone drilling projects has been to identify the most recent or most active slip surface. Effective tools for this task have been gas measurements, shear zone structures, mineralogy, and borehole logs such as caliper and seismic velocity. The active fault zone may be localized on site by continuous observation of the logging data and cores. However, the precise localization of the principal slip zone is not always obvious and careful microstructural studies of core samples are necessary to precisely determine the location and to extract important parameters related to the last earthquake (thickness of the principal slip zone, mineralogy, deformation mechanisms, and constitutive properties of fault gouge, slip weakening mechanisms, earthquake energy budget, and healing processes (see *Zoback et al., 2007*).

We recommend an integrated approach for future projects where real-time gas monitoring is combined with core analysis and borehole logs. Continuous coring with high recovery near the primary slip zone is necessary for the identification of the most recent slip zone using polished thin sections. Proper core handling procedures at the site, during transport and in the storage facilities, are critical to this stage of the operation as the microstructures are often extremely fragile. As the core often needs to be split into pieces to address multiple research topics, without the precise location of the major slip zone, integration of the studies becomes ambiguous. Accurate slip location is a prerequisite for interpretations in terms of earthquake rupture dynamics.



TCDP samples have induced a high international interest for friction experiments using soft rocks as initial material, and for slip-weakening processes in general. They have shown the lateral variability of the principal slip zone structure and thickness, the importance of clays, and mineralogy of the gouge for slip weakening during coseismic slip. The analysis from FMI and DSI logging also indicates variation of the stress orientation near the principal slip zone, suggesting a complete stress drop during faulting with the exchange of the orientation of the  $S_{H_{max}}$  to  $S_{h_{min}}$  [Wu *et al.*, 2007].

## Wenchuan

During the workshop, the Wenchuan Fault Zone Drilling Project began to drill (Figure 11). The first borehole was begun only 178 days after the devastating Mw7.9 May 12, 2008, earthquake.



**Figure 11.** Opening ceremony of the Wenchuan Fault Zone Drilling Project north of Dujiangyan.



**Figure 12.** Slip lines observed on the slip surface of the Corinth core.

The project plans four deep holes in the Wenchuan region funded by the Chinese government and is targeted close to the earthquake's epicenter. This latest fault zone drilling project has set a new record for rapid response and the workshop participants eagerly look forward to the results.

## Fault Zone Drilling Projects in the Absence of a Major Earthquake

### Corinth

The 1000-m-deep AIG10 well intersected, at around 760 m, the 10-km-long active Normal Aigion Fault in the Corinth Rift (western Greece). It was successful in providing cores of the fault zone, in particular the inner argillaceous layer that constitutes a hydraulic barrier in the direction perpendicular to the fault [Cornet *et al.*, 2004]. It also demonstrated that the normal stress to the fault at that depth is a principal component, as determined from the orientation of observed slip lines on slip surfaces (Figure 12) [Sulem, 2007]. Accurate pressure monitoring has suggested that large-magnitude ( $> 8$ ) distant teleseisms may trigger local slip instability. Downhole monitoring of high-frequency signals (2.5-kHz sampling rate) has demonstrated that the fault is the site of temporary high-frequency swarms that are believed to demonstrate a creeping deformation process of the fault in its upper domain. Development of regional microseismic swarm activity possibly linked to the creeping of the fault indicates that the cataclastic zones on both sides of the fault reach hydraulic transmissivity values in the  $10^4 \text{ cm}^2 \text{ sec}^{-1}$  range down to depths in the 7–8 km range. Monitoring the microseismic activity suggests that the fault becomes seismic below 3–4 km. The present plan is to explore the transition between creep and seismogenic behavior at around 3-km depth.

### SAFOD

The San Andreas Fault Observatory at Depth (SAFOD) was constructed as an element of the U.S. National Science Foundation EarthScope project, in conjunction with the U.S. Geological Survey, the National Aeronautics and Space Administration (NASA), International Continental Scientific Drilling Program (ICDP), and other organizations. SAFOD is located in central California at the transition between the creeping segment of the San Andreas Fault and the Parkfield segment, a section of the fault where seven moderate ( $\sim M6$ ) earthquakes have occurred since 1857, most recently on September 28, 2004. The Parkfield segment of the San Andreas Fault is the most densely instrumented fault

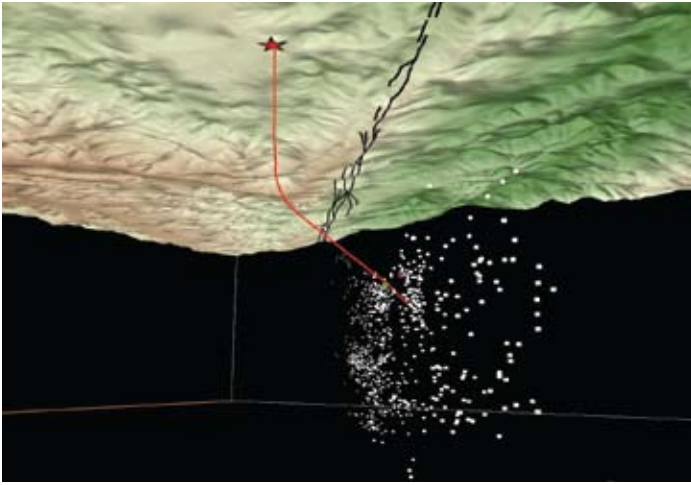


**Figure 13.** Perspective view of the SAFOD main hole (red) from below, showing the seismicity along the San Andreas Fault (white) and target repeating earthquakes. Topography and surface trace of the San Andreas Fault (black) shown from below. Illustration by L. Blair (USGS).

segment in the world. Seismic and deformation data from SAFOD are an integral part of the Parkfield earthquake experiment, as well as part of the EarthScope data repository.

The central scientific objective of SAFOD is to study the physical and chemical processes that control deformation and earthquake generation within an active plate-bounding fault zone. Through an integrated program of downhole sampling, measurements, and long-term monitoring, SAFOD was designed to: (1) determine the structure and properties of the fault zone at depth (2) utilize exhumed fault-zone core to determine the frictional behavior, physical properties, and chemical processes controlling faulting through laboratory analyses of fault rocks and fluids, (3) measure stress, permeability, and pore pressure conditions in situ, (4) characterize the three-dimensional volume of crust containing the fault, (5) directly monitor strain, pore pressure, and near-field seismic radiation during the cycle of repeating microearthquakes, and (6) observe earthquake nucleation and rupture processes in the near field.

The SAFOD pilot hole was drilled in 2002 to a depth of 2.2 km as a vertical hole located 1.8 km southwest of the surface trace of the San Andreas Fault. The pilot hole provided important technical information for engineering and drilling of the main hole through the fault. The SAFOD main hole, drilled as part of the EarthScope program in 2004, 2005, and 2007, began as a vertical hole and then deviated at  $\sim 60^\circ$  from vertical to the northeast using directional drilling techniques to pass below the surface trace of the fault at a vertical depth of 3 km (Figure 13). The rotary drilling in Phase 1 (2004) ended just weeks before the 2004 M6.0 Parkfield

earthquake, approximately 300 m short of the main active trace of the fault. Rotary drilling through the fault in 2005 (Phase 2) established access to the fault. Despite extremely difficult drilling conditions, the project successfully obtained a suite of sidewall cores and a comprehensive suite of open-hole logs prior to setting casing. Repeat measurements of the casing using a precise multi-finger caliper logging tool revealed two zones of progressive casing deformation that developed over the two-year hiatus between Phase 2 and Phase 3. In 2007, during Phase 3, the deformation zones were targeted for coring, and 39.9 m of core was successfully recovered. The core is being stored under carefully controlled conditions at the Integrated Ocean Drilling Program (IODP) Gulf Coast Repository at Texas A&M University. The core and other physical samples are NSF property and researchers wishing to work with them need to respond to NSF calls for proposals.

Following each drilling phase, seismometers were installed in the main hole to record nearby microearthquake activity. Earthquakes as close as 100 m to the instruments were successfully recorded. Using information from the borehole seismometers and temporary surface seismometers, it was possible to establish that the closest earthquakes recorded were located on one of the two actively creeping traces of the San Andreas Fault encountered in SAFOD. As the final step in the construction phase of SAFOD, observatory instrumentation was installed in the final core hole, approximately 150 m above the closest target earthquakes. The instruments currently in the well successfully recorded repeats of other nearby repeating earthquakes in December 2008 and additional aftershocks in January 2009. Data are available through the Northern California Earthquake Data Center at the University of California, Berkeley.

## NELSAM

The Natural Earthquake Laboratory in South African Mines (NELSAM) project is currently collecting high-frequency (up to 12 kHz) seismic data at 3.6-km depth and recording earthquakes in the magnitude range  $-3.0 < M_w < 3.0$  located meters to hundreds of meters from the seismometers. Using this data set, the NELSAM group continues to address critical issues concerning the earthquake source, including (1) the scaling of source parameters, such as apparent stress, stress drop, and rupture velocity, with seismic moment; (2) the partitioning of energy among radiated seismic, frictional, and fracture energies; (3) extent to which laboratory measurements can be applied directly to understand natural fault behavior; and (4) whether a minimum earthquake magnitude exists for a given tectonic environment. Thus far, their results show that some scaling exists between seismic signals in the early waveform and the final earthquake size [Lewis and Ben-Zion,

2008]. They determined that the Gutenberg-Richter distribution extends with no scale break to  $M_w -1.3$ , double-couple moment tensors for events as small as  $-2.2$ , and no evidence for a minimum magnitude [Boettcher *et al.*, submitted]. Peak ground velocity data can be used to determine maximum slip during an earthquake [McGarr *et al.*, submitted]. A subset of mining-induced earthquakes shows significant volumetric moment tensor components, which exhibit a transition from implosive to explosive components of the moment tensor with decreasing magnitude [Boettcher *et al.*, 2008]. Using observations from borehole breakouts and boundary element modeling, the project has also constrained the far-field stress state [Lucier *et al.*, 2009].

While the NELSAM experiment has, and will continue to obtain, abundant high-quality data directly from the earthquake source region, ultimately, the events recorded by NELSAM are mining-induced. To verify the applicability of NELSAM's results to naturally occurring earthquakes, we need to compare our findings to high-quality seismic data from the hypocentral region an active tectonic fault.

In conclusion, each drilling program has provided its own set of answers to some scientific questions on fault zone geology because of the different nature of parent rocks, dynamic context, and volume of fluids involved in faulting. More information is still needed on the friction, earthquake interaction, healing processes, and material properties on the fault.

# IV. Proposed Earthquake Drilling Plan

Rapid drilling entails rapid decision making. An important goal of the Rapid Response Drilling Workshop was to develop a drilling plan that can serve as a blueprint for future rapid response operations. All of the participants were cognizant of the variety of situations likely to be encountered in the real world and understand that no pre-earthquake drilling plan will be appropriate in detail for any particular situation. However, having a scenario drilling plan that specifically addresses the key scientific questions may provide future projects with a useful starting point for the work in the critical time following an earthquake.

## Key Observables in a Rapid Response Borehole

Section II described the key measurements required in a scenario drilling plan for a rapid response borehole, which would provide answers to some fundamental questions of earthquake science. Briefly, these measurements include:

- **Repeat temperature logs, with a precision of +/- 10 mK.** Repeated temperature logs are required to distinguish between the signal of frictional heating and other potential sources of curvature in the geotherm, including variations in thermal properties, and the advective effects of drilling and fluid flow.
- **Stress measurements.** Downhole stress measurements will provide information about the magnitude of stresses in the near field of the fault following an earthquake.
- **Coring across the fault zone.** Coring across the fault zone is required to define fault architecture, fabric, composition, grain size, and deformation mechanisms; to obtain material for laboratory measurements of mechanical, hydrologic, and thermal properties; and to characterize basic physical properties on site. These data do not need to be generated through the entire borehole, but from ~ 100 m above to ~ 100 m below the fault zone.
- **Geophysical logging.** Imaging, density, caliper, and seismic velocity logs are critical to defining fault zone architecture, as well as for establishing a baseline for studies of fault and damage zone healing.
- **Repeat hydrologic perturbation testing.** Hydrologic draw-down or injection tests (conducted in a packed, sealed fault interval) are needed to evaluate fault zone permeability and its changes following an earthquake.
- **Repeat active-source seismic experiments (VSP).** Active controlled-source seismic experiments conducted with instruments downhole will be needed to characterize changes in wall rock and the fault zone associated with the time-dependent healing processes.
- **Sampling of mud gas and fluids.** Geochemical sampling should include mud gas analysis during drilling and downhole sampling of fluids for major ion chemistry immediately following drilling to obtain a geochemical “baseline”; repeated fluid sampling at later times (likely in conjunction with hydrologic tests) is required to evaluate chemical aspects of fault healing processes.
- **Continuous, long-term monitoring of temperature and pore fluid pressure.** Continuous monitoring is desirable to obtain high-resolution time series of temperature (as a function of depth) and pore pressure within the fault zone. These measurements will help to distinguish between advective diffusive heat transport mechanisms, in order to constrain frictional heating (e.g., Figure 2). Pore pressure monitoring is also needed to define fault zone pore fluid pressure and its evolution after an earthquake; the response to Earth tides provides an additional measure of rock properties (stiffness and permeability) and their evolution. Temperature measurements should be made to a precision of +/- 10 mK, and pore pressure to +/- 10 Pa at 1 Hz or higher frequency.
- **Passive seismic.** A combination of downhole seismometers and surface stations are required to locate earthquakes, record their kinematics close to the source, and capture their interactions.

In addition to the above field measurements, laboratory studies and modeling work must be done throughout the project. The sooner these complementary studies are begun, the more they can help guide the data collection process. Both modeling and laboratory techniques should be considered integral to the drilling operation.

## Site Selection Criteria

Rapid response drilling should be considered whenever there is a large, on-land earthquake with sufficient surface slip ( $> 1$  m) to generate large geophysical and geological anomalies at depths that could be accessible to a drilling program. The actual earthquakes that will be targeted in practice will in large part be determined by the local scientific and technical infrastructure. Box F discusses some plausible targets that are likely to have an earthquake suitable for deep drilling in the near future.

Once such an earthquake happens, several basic drilling-site selection requirements are aimed at addressing fundamental questions about earthquake energy budgets and fault zone processes. First, it is desirable to drill where the fault and regional geologic structure are well known and relatively simple. A single major fault strand rather than multiple active traces will provide data that are more easily interpretable in the context of large-scale seismological information. Second, drilling should target a region of high co-seismic slip on the fault, as defined by seismological inversions and surface deformation data. Slip should be at least 1 m at the drilling site in order to ensure a measurable frictional signal. Ideally, the drilling would reach nucleation depths, although this is unlikely to be feasible in many cases and thus most drilling projects will concentrate on the problems of friction, healing, and earthquake interaction. Third, crystalline rock is preferred over sedimentary rock because of its low permeability, and its well-defined frictional properties. Unconsolidated sediments are particularly problematic for studying the seismogenic zone. Fourth, a dipping fault is ideal (though not required) because it would allow crossing the fault at a high angle to the structure within a vertical borehole. The scenario drilling plan described here assumes a dipping fault. Finally, it would be desirable to drill in a location where there are numerous pre-existing seismological and GPS stations, though again this is not a requirement.

## Drilling Strategy

A significant challenge in designing and implementing a scenario drilling plan is coordination of multiple desired downhole measurements and instrument installations, due to competition for limited space in the hole, and potentially interfering effects. These multiple objectives must be spatially and temporally balanced, requiring careful: (a) design and completion strategy, including planning of measurement sequences to minimize interference; and (b) prioritization and compromise of some measurements (e.g., running only low-volume perturbation tests for stress and hydrologic measurement objectives, or conducting only limited coring).

The key measurements enumerated above each carry specific hole configuration and/or timing requirements, which must be taken into consideration in designing a drilling strategy. Specifically:

- Temperature logging requires an open conduit from the surface to total depth, or removal of other instruments emplaced in the hole for each temperature logging run. Instrument removal may require re-equilibration of fluids post-emplacment and may introduce undesirable offsets in measurements.
- Hydrologic testing requires hydraulic isolation of the test interval (fault zone) by packers or cement.
- Seismometer, strainmeter, and/or tiltmeter installations require coupling to the formation via cement or clamping.
- Geochemical measurements should be conducted soon after—or during—drilling for mud gas and major ion chemistry, to provide a baseline for any changes associated with healing.
- Large volumes of fluid withdrawal or injection may perturb the thermal and chemical regimes locally, and are thus undesirable. It is likely that injection testing would disturb conditions more than withdrawal testing. This dilemma places a constraint on the type and number of stress measurements (e.g., leak-off or mini-frac tests) and hydraulic perturbation experiments.

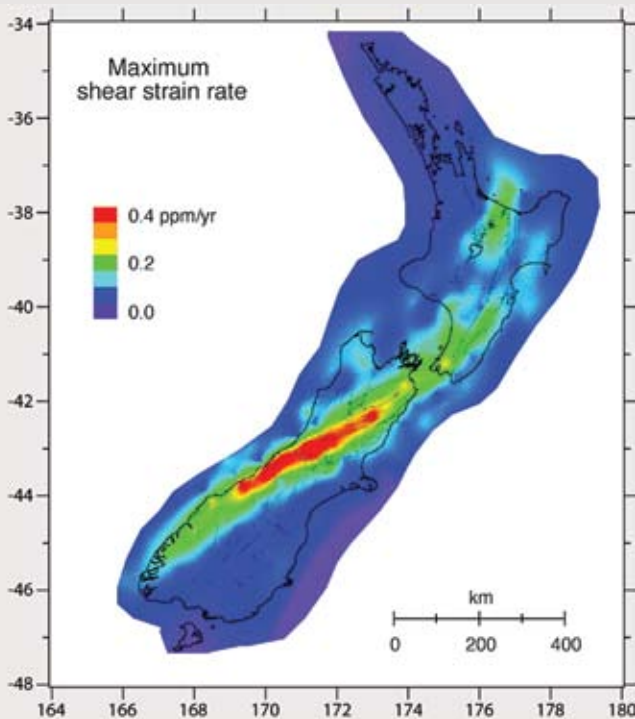
## Scenario Drilling and Completion Plan

Reconciling the conflicting requirements of multiple measurements is one of the most challenging aspects of a drilling project. Below we provide a sample drilling plan to illustrate how the competing projects can be balanced in a realistic scenario. The workshop together developed a “straw man” scenario drilling plan that can accommodate most of the key measurements needed to address fundamental questions about the earthquake energy budget and fault healing. This drilling plan describes a basic sequence of drilling, downhole measurements and coring, and hole completion operations, but does not include fine technical details, cost, or drilling time estimates. This sequence is described below, and shown schematically in Figure 14.

One key consideration in defining a target drilling depth is the minimum depth required to obtain meaningful information about frictional heating. Getting the needed information depends on instrument resolution and the magnitude of the expected thermal anomaly (based on average shear stress during slip and the total amount of slip) (c.f. Figure 1c). As discussed earlier, there is a



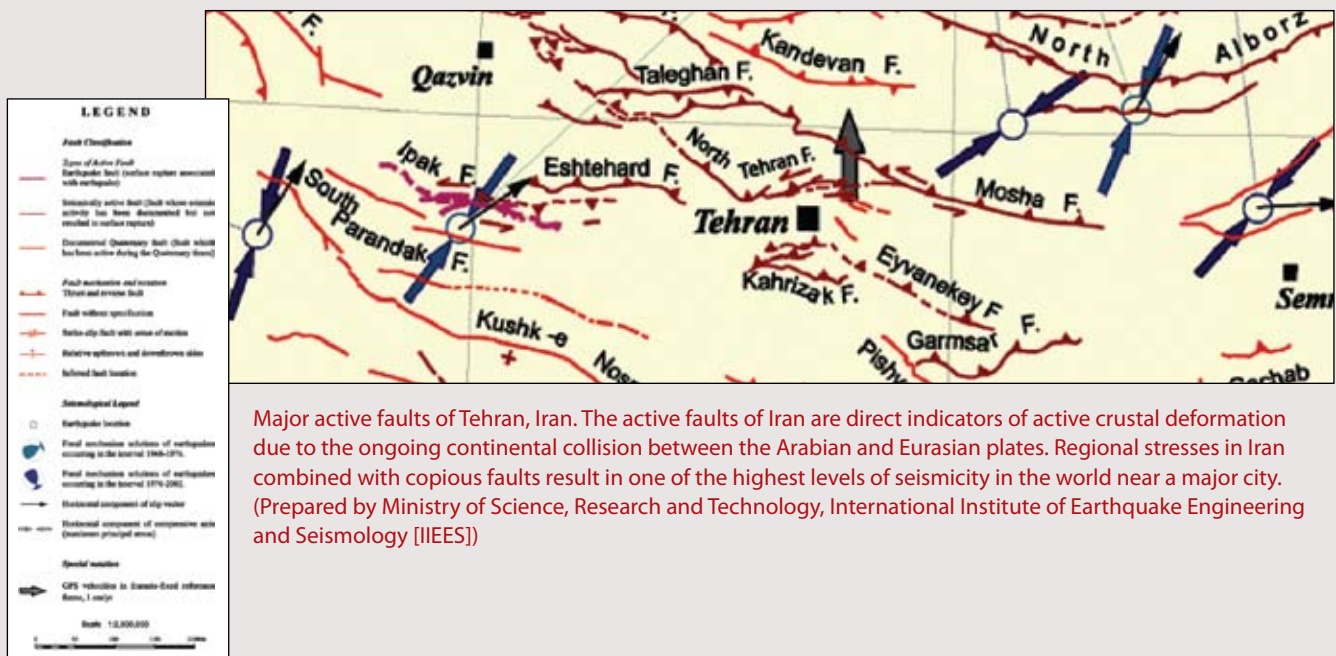
Box F continued...



Strain rate accumulation in New Zealand indicates the mature Alpine Fault on the South Island is likely to have a major earthquake. The extensive strike-slip fault is unusual in having a dip of  $\sim 50^\circ$ , which allows vertical drilling into the slip zone. Preliminary plans are already under way for a drilling project in the region (from *Beavan and Haines [2001]*).



In addition to its famous subduction zone seismicity, Japan has on-land earthquakes with large offset. Shown here is vertical offset of about 3 m at the Himawari Park in Nagano city, about 150 km northwest of Tokyo, Japan, formed during the 1854 Zenkoji earthquake (Mw7.4) on a thrust fault shown above (although its original surface has been artificially modified). Since 1854, such a large vertical offset due to a shallow thrust earthquake occurred in 1896 (Mw6.9) and 1945 (Mw6.6) in Japan.



Major active faults of Tehran, Iran. The active faults of Iran are direct indicators of active crustal deformation due to the ongoing continental collision between the Arabian and Eurasian plates. Regional stresses in Iran combined with copious faults result in one of the highest levels of seismicity in the world near a major city. (Prepared by Ministry of Science, Research and Technology, International Institute of Earthquake Engineering and Seismology (IIEES))

tradeoff between these considerations and when drilling begins after an earthquake. For a suite of conservative assumptions about heat generation, a 2-km-deep hole drilled within six to 12 months following an earthquake is sufficient; deeper drilling is better, but the time and cost increase exponentially with increased depth (See Box D). This depth range is also adequate for the desired geophysical measurements. The scenario drilling plan described here is based on planning for a 2-km-deep hole, penetrating a fault within a high-slip zone at 1750-m vertical depth. This plan and general completion strategy could be adjusted for any target fault depth, although the details of casing set points and sizes would need to be modified.

The first set of operations would drill the hole with full bore rotary drilling, logging to ~2000-m vertical depth, with continuous rotary coring from ~1600 to ~1850 m (from 150 m above to 100 m below the target fault) and with real-time mud gas logging and cuttings collection throughout the borehole. Several casings will need to be set along this drilling path; typically, this includes a 24" or 18.65" standpipe to a depth of ~50 m for wellhead support, followed by intermediate and cemented casings to the surface as required by drilling conditions. The scenario plan includes a casing setting point at 1600 m (above the fault zone) before switching over to coring, with 9.65" or 7" outer diameter (OD) pipe. The drilling sequence would require a pipe trip to switch from rotary to coring assemblies at 1600 m. Basic core analysis and description should be conducted on site and immediately upon core recovery, if possible. In the event "logging while drilling" data acquisition (LWD) is planned and warranted by the drilling conditions, the instrument string should include, at a minimum, density, gamma, resistivity at bit, and sonic tools. The core should be rapidly transported to a climate-controlled preservation facility. Proper refrigeration and humidity control of the core is necessary to preserve the fragile structures of the fault zone and formation pore waters and saturation state (Box E).

After drilling, if hole conditions permit, a series of logging runs should be conducted in the following priority order: (1) wireline logging for temperature, resistivity, including imaging (FMI), density, gamma ray, fluid sampling, and sonic velocity; and (2) stress measurements via a dual-packer modular formation dynamics tester (MDT) tool or equivalent, using the minimum possible fluid-injection rates.

Following these operations, the hole should be cased to total depth. Casing installation limits the possibility for repeated stress measurements or geochemical fluid sampling distributed downhole, but is required all other monitoring and downhole objectives. After cementing the casing to a depth well above to fault target, a

cement bond and temperature logging run should be conducted to verify the top of cement. Quality of the cement is particularly critical to fluid hydrogeological operations. After the logging runs are completed, the casing and cement would be perforated at the fault zone to enable long-term hydrologic monitoring and perturbation testing in the fault zone. Immediately after casing perforation, a temperature logging run would be useful to rapidly discern whether the fault is hydrologically active.

At this time, the hole would be readied for long-term monitoring installation. The scenario plan here calls for the assembly of a surface wellhead with a pressure-tight monitoring cable outlet from the last cemented casing annulus, as well as installation of an open, removable small-diameter (2.875" or 3.5") tubing extending to ~ 1900-m vertical depth to be hung at the wellhead. This tubing would provide the access conduit for continuous temperature monitoring via a distributed thermistor string, as well as for repeat temperature logging. Outside of the tubing, a packer element set above the fault target (1700–1710 m) would hydraulically isolate the perforated fault zone interval; the packer would need to accommodate pass-throughs for fluid sampling and for a data cable from a pore pressure transducer (Figure 14 panel D). If possible, an array of short-period seismometers could be included as part of the sensor assembly; these instruments would be on the outside of the tubing, and clamped to the inner diameter of the casing. Immediately after installing the tubing, temperature logs would be collected, followed by a low-volume pump test in the fault zone, followed immediately by a second temperature logging run to assess the effects of the hydrologic perturbation test on temperatures. If seismometers are installed on the outside of the tubing, a VSP experiment could then be conducted; preferably it would include both zero-offset and long-offset components.

After this phase of installation and active testing, the hole would equilibrate for several months. During this time, repeat temperature logs could be collected inside the tubing at any desired time interval without impacting any other components of the installation. Similarly, repeated geophysical experiments could be conducted as desired and recorded by the downhole array. After about six months, a second small-volume pump test would be conducted, immediately preceded and followed by temperature logging runs as for the first perturbation test. The exact timing of this experiment should be selected on the basis of results from the initial test, which will define the thermal effects and relaxation time of the first small-volume hydrologic perturbation. The pumped fluids would be retained and analyzed for major and trace element geochemistry for comparison with the baseline data set. These operations could then be repeated as desired.

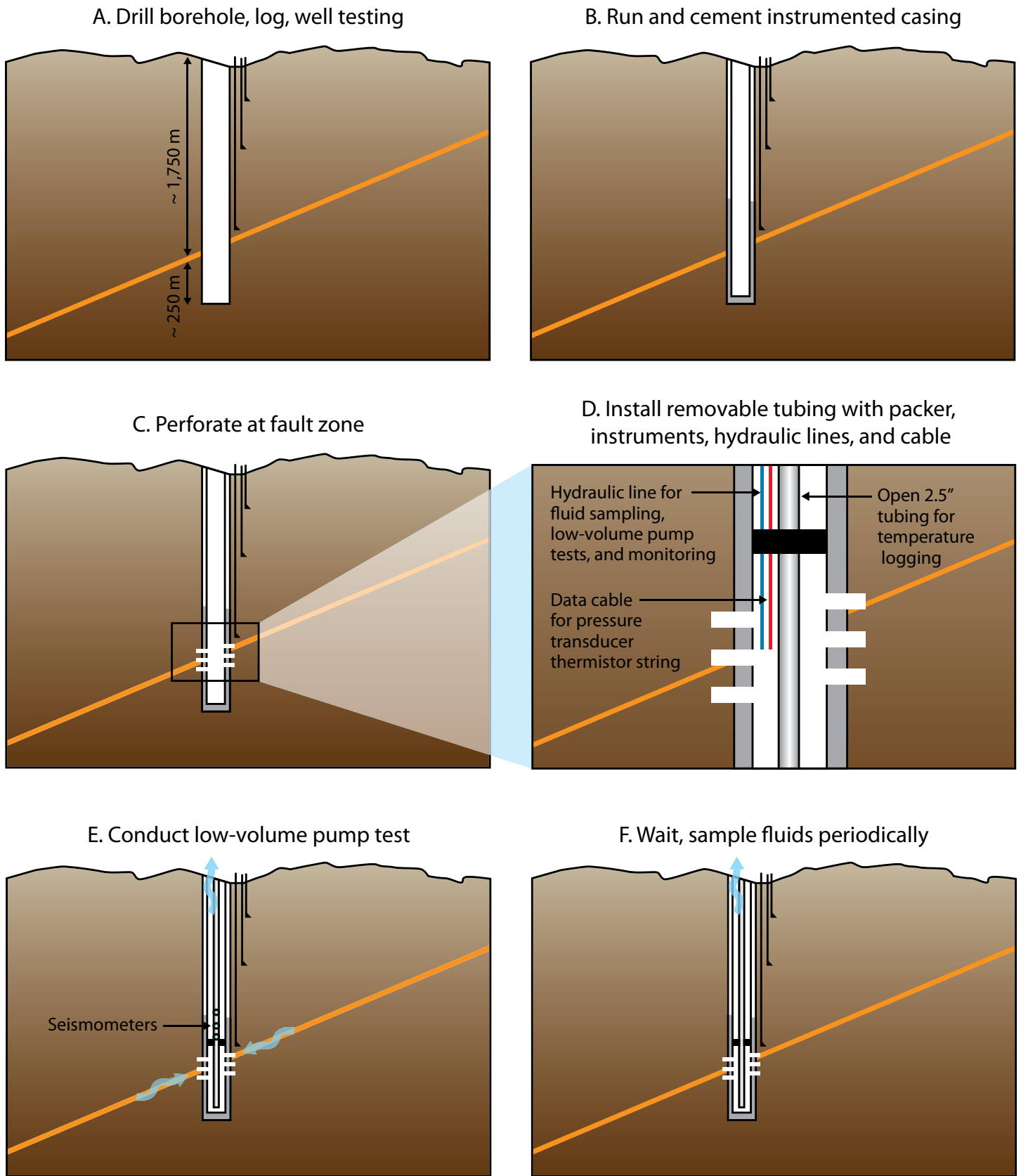


Figure 14. Schematic of a rapid drilling plan.

## BOX G. Instrument Development Needs for Deep Boreholes

At present, readily available borehole geophysical instruments and their installations for earthquake studies can be divided into several types. The types are based on their combination of downhole temperature and pressure specifications, and active or passive sensors and downhole electronics. Constraints in this choice are driven by borehole diameter, pressure, and temperature, with temperature the most difficult concern.

Currently, in standard-size drillholes, off-the-shelf passive sensors and cables connected to surface electronics can readily be made to work long term to depths of several kilometers and temperatures on the order of  $\sim 150^{\circ}\text{C}$ . On the other hand, the cutoff for the long-term operation of off-the-shelf active (digital) sensors and/or downhole electronics is nominally less than about  $\sim 75^{\circ}\text{C}$ .

The near-surface instruments and installations have relatively high success rates. For example, of the 79 EarthScope Plate Boundary Observatory (PBO) installations at  $\sim 250\text{-m}$  depth, 100% of the passive seismometers and nearly 80% of the active strainmeters are operating within specifications. Further, most of the suboperational strainmeters have coupling and installation issues, not electronic ones, related to the complicated way these instruments must be coupled to the borehole.

In deeper and hotter boreholes, passive instruments have had success in many places, including Japan, Switzerland, and California, where passive sensors continue to work long term in  $100\text{--}150^{\circ}\text{C}$  conditions at depths of 3 km. However, even in these cases, system lifetimes have been found to be limited to several years and further development is warranted.

Experience with active instruments in deeper and hotter boreholes is currently much more limited, especially in noncommercial spheres. In these cases, it has been found that such instruments have much higher and rapid failure rates than passive ones. The problems are complex, and long-term operations in these circumstances have been accomplished only by maintaining the ability to withdraw and replace the instrument and cable on a regular basis.

For realistic rapid scientific borehole response to a major earthquake, a stock of passive systems designed for depths of a few kilometers and temperatures of  $150^{\circ}\text{C}$  is readily achievable. It is also clear that digital instruments are necessary to accomplish the goals of deep hole projects and that further development must be continued in anticipation of these activities to achieve more robust, deep sensors and cabling

# V. Recommendations

The key recommendation of the workshop is that rapid response drilling should be priority of the international drilling community in response to any earthquake that occurs with more than 1 m of slip on land in a region with sufficient infrastructure to support the technical operations. The optimal drill site is on crystalline rock with a dipping fault and well-characterized geology. The hole should be initiated within six months after the earthquake and be drilled to a depth of at least 2 km.

To achieve this goal, the workshop participants recommend the following courses of action for ICDP and the scientific community.

## Recommendations for ICDP

- ICDP should form a standing committee on fault drilling.
- A mechanism should be created to facilitate rapid evaluation and funding of scientific drilling proposals immediately following an earthquake.
- Fault zone drilling projects should include a contingency plan for accelerating or reconfiguring the project in case of a major earthquake.
- An inventory of baseline data on and near major faults should be constructed under the supervision of the standing committee as soon as possible for reference information before an earthquake occurs. The inventory should include existing, accessible borehole, current seismological and geodetic instrumentation, and paleoseismic constraints. As part of this process, geophysical logging should be conducted on extant boreholes in strategic locations near major faults.
- An emergency response kit should be built and maintained by ICDP, including material stockpiles and borehole instrumentation, including special downhole tools.
- Investments should be made into developing and improving sensors for deep, hot adverse fault zone environments.

## Recommendations for the Scientific Community

- National and regional groups should form and work on scenario plans for their localities. Having clear and accurate geological and geophysical maps prior to a major earthquake are critical for optimally selecting a study site after the earthquake.
- Complementary seismological and geological studies at potential sites of large earthquakes should be undertaken now. Existing boreholes should be logged. Baseline data are critical to post-earthquake interpretation.

# Appendix.

## Workshop Participants

Serif **BARIS**, Kocaeli University, Turkey

Margaret **BOETTCHER**, University of New Hampshire, USA

Ann-Marie **BOUILLIER**, Grenoble University, France

Emily **BRODSKY**, University of California, Santa Cruz, USA

Mai-Linh **DOAN**, Grenoble University, France

Bill **ELLSWORTH**, US Geological Survey, USA

Jorge **ERZINGER**, GFZ Deutches, Germany

François **CORNET**, University de Strasbourg, France

Naoyuki **FUJII**, Shizuoka University, Japan

Patrick **FULTON**, Oregon State University, USA

Hongkui **GE**, Chinese Earthquake Administration, China

Robert **HARRIS**, Oregon State University, USA

Fuqing **HUANG**, Chinese Earthquake Administration, China

Bor-shuah **HUANG**, Academia Sinica, Taiwan

Satoshi **IDE**, Earthquake Research Institute, Tokyo University,  
Japan

Barbara **JOHN**, University of Wyoming, USA

Maria Jose **JURADO**, Institute of Earth Sciences-CSIC Barcelona,  
Spain

Hiroo **KANAMORI**, California Institute of Technology, USA

Yasuyuki **KANO**, Disaster Prevention Research Institute, Kyoto  
University, Japan

Kate **SCHARER**, Appalachian State University, USA

Achim **KOPF**, Bremen University, Germany

Shin'ichi **KURAMOTO**, JAMSTEC, Japan

Yong-gang **LI**, University of Southern California, USA

Weirin **LIN**, JAMSTEC, Japan

Kuo-Fong **MA**, National Central University, Taiwan

Peter **MALIN**, University of Auckland, New Zealand

Norio **MATSUMOTO**, Geological Survey of Japan, Japan

David **MENCIN**, UNAVCO, USA

Casey **MOORE**, University of California, Santa Cruz, USA

Jim **MORI**, Disaster Prevention Research Institute, Kyoto  
University, Japan

John **NABELEK**, Oregon State University, USA

Berhard **PREVEDELL**, ICDP, Germany

Demian **SAFFER**, Pennsylvania State College, USA

Serge **SHAPIRO**, Freie University of Berlin, Germany

Toshihiko **SHIMAMOTO**, Hiroshima University, Japan

Kiyoshi **SUYEHIRO**, JAMSTEC, Japan

Hidemi **TANAKA**, Tokyo University, Japan

Harold **TOBIN**, University of Wisconsin, USA

Sonata **WU**, Stanford University, USA

Zhiqin **XU**, Chinese Academy of Geological Sciences, China

Yasuhiro **YAMADA**, Kyoto University, Japan

Makata **YAMANO**, Earthquake Research Institute, University of  
Tokyo, Japan

Mahmoud **YAZDANI**, Tarbiat Modares University, Iran

Lingsen **ZENG**, Chinese Academy of Geological Sciences, China

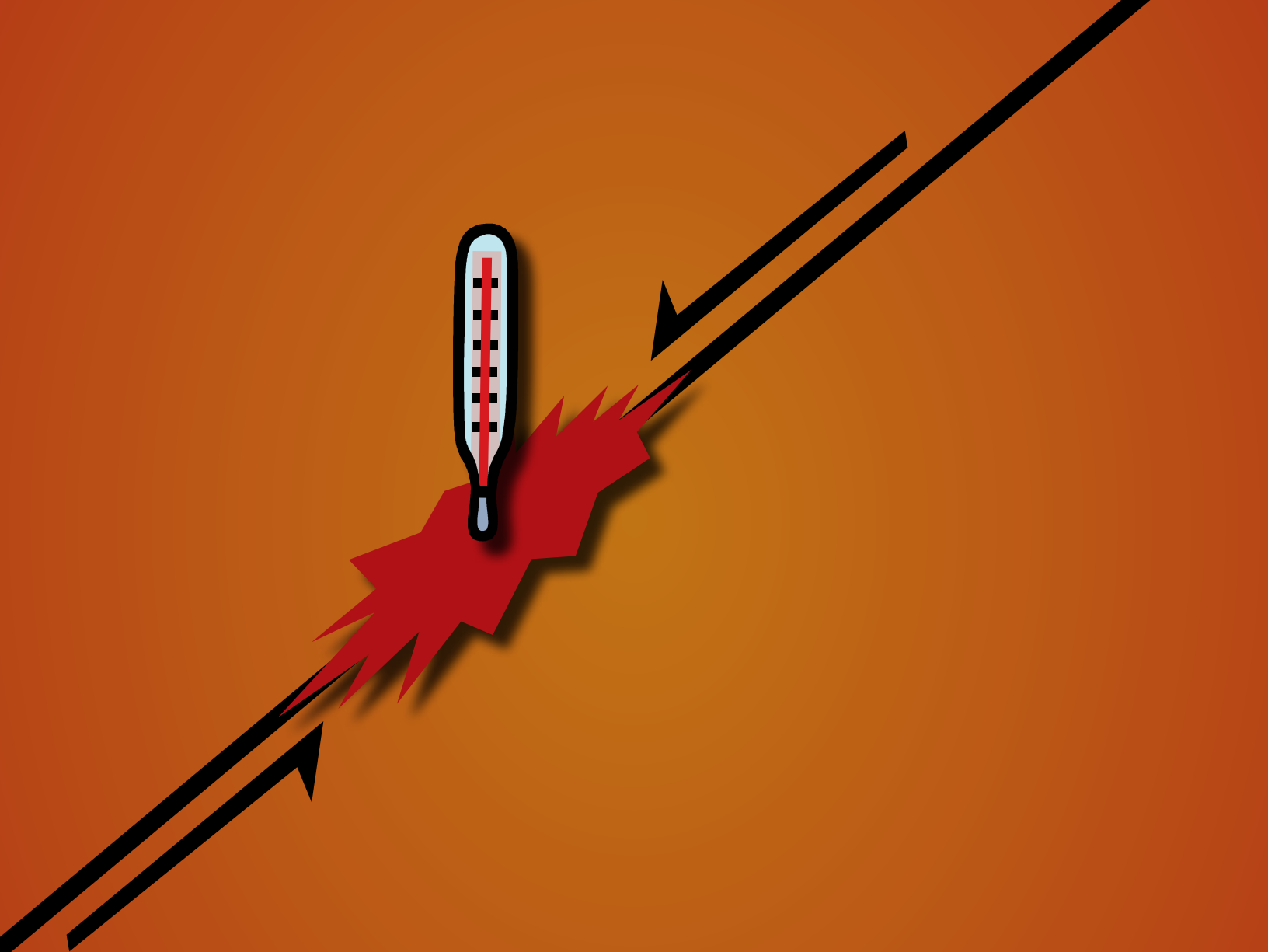
# References

- Andrews, D.J., 2002, A fault constitutive relation accounting for thermal pressurization of pore fluid, *J. Geophys. Res.*, 107(B12), 2363, doi:10.1029/2002JB001942.
- Beavan, J., and J. Haines, 2001, Contemporary horizontal velocity and strain rate fields of the Pacific-Australian plate boundary zone through New Zealand, *J. Geophys. Res.*, 106, 741–770.
- Boettcher, M.S., A. McGarr, and M. Johnston. Minimum-magnitude earthquakes in South African gold mines: Implications for earthquake nucleation, submitted to *Geophys. Res. Lett.*
- Boettcher, M.S., A. McGarr, R.J. Durrheim, S. Spottiswoode, A. Milev, L. Linzer, M.J.S. Johnston, and R.W. Sell, 2008, A broadband, wide dynamic range investigation of earthquakes in deep South African gold mines, *Seismol. Res. Lett.*, 79(2), 311.
- Boullier, A.M., T. Ohtani, K. Fujimoto, H. Ito, and M. Dubois, 2001, Fluid inclusions in pseudotachylytes from the Nojima fault, Japan, *Journal of Geophysical Research Solid Earth*, 106 (B10), 21,965–21,977.
- Boullier, A.-M., E.-C. Yeh, S. Boutareaud, S.-R. Song, and C.-H. Tsai, *in press*, Microscale anatomy of the Chi-Chi earthquake fault zone, *Geochemistry, Geophysics, and Geosystems*, doi:2008GC002252.
- Boullier, A.M., K. Fujimoto, H. Ito, T. Ohtani, N. Keulen, O. Fabbri, D. Amitrano, M. Dubois, and P. Pezard, 2004a, Structural evolution of the Nojima fault (Awaji Island, Japan) revisited from the GSJ drill hole at Hirabayashi, *Earth Planets and Space*, 56 (12), 1233–1240.
- Boullier, A.M., K. Fujimoto, T. Ohtani, G. Roman-Ross, E. Lewin, H. Ito, P. Pezard, and B. Ildefonse, 2004b, Textural evidence for recent co-seismic circulation of fluids in the Nojima fault zone, Awaji island, Japan, *Tectonophysics*, 378, 165–181, doi:10.1016/j.tecto.2003.09.006.
- Boutareaud, S., A.M. Boullier, P. Beck, D.-G. Calugaru, R. Han, and A. Tsutsumi, 2008, Clast-clay aggregates as new indicator of shallow crustal seismic slips, *Geophysical Research Abstracts*, 10, 1607–7962/gr/EGU2008-A-04694.
- Brenguier F., M. Campillo, C. Hadziioannou, N.M. Shapiro, R.M. Nadeau, and E. Larose 2008, Postseismic Relaxation Along the San Andreas Fault at Parkfield from Continuous Seismological Observations, *Science*, 321, 1478–1481.
- Brodsky, E.E., and H. Kanamori, 2001, The elastohydrodynamic lubrication of faults, *J. Geophys. Res.*, 106, 16357–16374.
- Brodsky, E.E., C.D. Rowe, F. Manighenni, and J. C. Moore, 2009, A geological fingerprint of extremely low viscosity fault fluids during an earthquake, *J. Geophys. Res.*, 114(B01303), doi:10.1029/2008JB005633.
- Brune, J.N., T.L. Henyey, and R.F. Roy, 1969, Heat flow, stress, and rate of slip along the San Andreas Fault, California, *J. Geophys. Res.*, 74(15), 3821–3827.
- Chen, K.C., B.S. Huang, J.H. Wang, W.G. Huang, T.M. Chang, R.D. Hwang, H.C. Chiu, and C.C.P. Tsai, 2001, An observation of rupture pulses of the 20 September 1999 Chi-Chi, Taiwan, earthquake from near-field seismograms, *Bull. Seism. Soc. Am.*, 91 (5), 1247–1254.
- Cornet F.H., M.L. Doan, I. Moretti, G. Borm, 2004, Drilling through the active Aigion Fault : The AIG10 well observatory, *Compt. Rendus Geosci.*, 336(4–5), 395–406.
- Dixon, T. H., and J. C. Moore (Eds.), 2007, *The Seismogenic Zone of Subduction Thrust Faults*, Columbia Univ. Press, 680 pp.
- Doan, M.-L., E.E. Brodsky, Y. Kano, and K.-F. Ma, 2006, In-situ measurement of the hydraulic diffusivity of the active Chelungpu Fault, Taiwan, *Geophys. Res. Lett.*, 33, L16317, doi:10.1029/2006GL026889.
- Elkhoury, J., E.E. Brodsky, and D.C. Agnew, 2006, Seismic waves increase permeability, *Nature*, 441, 1135–1138.
- Felzer, K.R., R.E. Abercrombie, and G. Ekstrom, 2004, A common origin for aftershocks, foreshocks, and multiplets, *Bull. Seism. Soc. Am.*, 94, 88–98.
- Fuis, G.S., 2008. The San Andreas fault in southern California has a “propeller” shape – implications for tectonic and seismic hazard, *Geological Society of America Abstracts with Programs*, 40, 326.
- Fujimoto, K., A. Ueda, T. Ohtani, M. Takahashi, H. Ito, H. Tanaka, and A.-M. Boullier, 2007, Borehole water and hydrologic model around the Nojima fault, SW Japan, *Tectonophysics*, 443, 174–182.
- Fulton, P.M., D.M. Saffer, and E.E. Brodsky, 2008, The role of advection on fault zone temperature after an earthquake: Implications for rapid response drilling, *Eos Trans. AGU*, 89(52), Fall Meet. Suppl., Abstract T53F-05.
- Geraud, Y., M. Diraison, and N. Orellana, 2006, Fault zone geometry of a mature active normal fault: A potential high permeability channel (Pirgaki fault, Corinth rift, Greece), *Tectonophysics*, 426(1–2), 61–76.
- Hashimoto, Y., O. Tadaï, M. Tanimizu, W. Tanikawa, T. Hirono, W. Lin, T. Mishima, M. Sakaguchi, W. Soh, S.-R. Song, K. Aoike, T. Ishikawa, M. Murayama, K. Fujimoto, T. Fukuchi, M. Ikehara, H. Ito, H. Kikuta, M. Kinoshita, K. Masuda, T. Matsubara, O. Matsubayashi, M. Mizoguchi, N. Nakamura, K. Otsuki, T. Shimamoto, H. Sone, and M. Takahashi, 2008, Characteristics of chlorites in seismogenic fault zones: The Taiwan Chelungpu Fault Drilling Project (TCDP) core sample, *e-Earth*, 3 (<http://www.electronic-earth.net/3/issue1.html>), 1–6.
- Helmstetter, A., Y.Y. Kagan, and D.D. Jackson, 2005, Importance of small earthquakes for stress transfers and earthquake triggering, *J. Geophys. Res.*, 110, B05S08.
- Hickman, S., R. Sibson, and R. Bruhn, 1995, Introduction to special section: Mechanical involvement of fluids in faulting, *J. Geophys. Res.*, 100, 12,831–12,840.
- Hiramatsu, Y., H. Honma, A. Saiga, M. Furumoto, and T. Ooida, 2005, Seismological evidence on characteristic time of crack healing in the shallow crust, *Geophys. Res. Lett.*, 32(9), L09304.
- Hirono, T., W. Lin, E.C. Yeh, W. Soh, Y. Hashimoto, H. Sone, O. Matsubayashi, K. Aoike, H. Ito, M. Kinoshita, M. Murayama, S.R. Song, K.F. Ma, J.H. Hung, C.Y. Wang, and Y.B. Tsai, 2006, High magnetic susceptibility of fault gouge within Taiwan Chelungpu fault: Nondestructive continuous measurements of physical and chemical properties in fault rocks recovered from Hole B, TCDP, *Geophys. Res. Lett.*, 33, L15303, doi:10.1029/2006GL026133.
- Hirono, T., E.C. Yeh, W. Lin, H. Sone, T. Mishima, W. Soh, Y. Hashimoto, O. Matsubayashi, K. Aoike, H. Ito, M. Kinoshita, M. Murayama, S.R. Song, K.F. Ma, J.H. Hung, C.Y. Wang, Y.B. Tsai, T. Kondo, M. Nishimura, S. Moriya, T. Tanaka, T. Fujiki, L. Maeda, H. Muraki, T. Kuramoto, K. Sugiyama, and T. Sugawara, 2007a, Non-destructive continuous physical property measurements of core samples recovered from hole B, Taiwan Chelungpu-Fault Drilling Project, *J. Geophys. Res.*, 112, B07404, doi:10.1029/2006JB004738.
- Hirono, T., T. Yokoyama, Y. Hamada, W. Tanikawa, T. Mishima, M. Ikehara, V. Famin, M. Tanimizu, W. Lin, W. Soh, and S.R. Song, 2007b, A chemical kinetic approach to estimate dynamic shear stress during the 1999 Taiwan Chi-Chi earthquake, *Geophys. Res. Lett.*, 34(L19308), doi:10.1029/2007GL030743.
- Hirono, H., M. Sakaguchi, K. Otsuki, H. Sone, K. Fujimoto, T. Mishima, W. Lin, W. Tanikawa, M. Tanimizu, W. Soh, E.C. Yeh, and S.R. Song, 2008, Characterization of slip zone associated with the 1999 Taiwan Chi-Chi earthquake: X-ray CT image analyses and microstructural observations of the Taiwan Chelungpu fault, *Tectonophysics*, 449, 63–84, doi: 10.1016/j.tecto.2007.12.002.

- Hubbert, M.K., and W.W. Rubey, 1959, Role of fluid pressure in mechanics of overthrust faulting, *Bull. Geol. Soc. Amer.*, 70, 115–166.
- Hung, J.H., Y.H. Wu, E.C. Yeh, J.C. Wu, and T.S. Party, 2007, Subsurface structure, physical properties, and fault zone characteristics in the scientific drill holes of Taiwan Chelungpu-fault Drilling Project, *Terrestrial, Atmospheric and Oceanic Sciences*, 18(2), 271–293.
- Ikeda, R., 2001a, Outline of the fault zone drilling project by NIED in the vicinity of the 1995 Hyogo-ken Nanbu earthquake, Japan, *Island Arc*, 10, 199–205.
- Ikeda, R., Y. Iio, and K. Omura, 2001b, In situ stress measurements in NIED boreholes in and around the fault zone near the 1995 Hyogo-ken Nanbu earthquake, Japan, *Island Arc*, 10, 252–260.
- Ishikawa, T., M. Tanimizu, K. Nagaishi, J. Matsuoka, O. Tadai, M. Sakaguchi, T. Hirono, M. Mishima, W. Tanikawa, W. Lin, H. Kikuta, W. Soh, and S.-R. Song, 2008, Coseismic fluid–rock interactions at high temperatures in the Chelungpu fault, *Nature Geoscience*, 1, 679–683.
- Kanamori, H., and E.E. Brodsky, 2004, The physics of earthquakes, *Reports on Progress in Physics*, 67, 1429–1496.
- Kano, Y., J. Mori, R. Fujio, H. Ito, T. Yanagidani, S. Nakao, and K.-F. Ma, 2006, Heat signature on the Chelungpu fault associated with the 1999 Chi-Chi, Taiwan earthquake, *Geophys. Res. Lett.*, 33, L14306, doi:10.1029/2006GL026733.
- Kitagawa, Y., K. Fujimori, and N. Koizumi, 2002, Temporal change in permeability of the rock estimated from repeated water injection experiments near the Nojima fault in Awaji Island, Japan, *Geophys. Res. Lett.*, 29, 1483.
- Kuo, L.W., S.R. Song, and H.Y. Chen, 2005, Characteristics of clay mineralogy in the fault zone of the TCDP and its implication, *Eos Trans. AGU, Fall Meet. Supp.*, 86 (52), Abstract T43D-05.
- Lachenbruch, A.H., and J.H. Sass, 1980, Heat flow and energetics of the San Andreas fault zone, *J. Geophys. Res.*, 85, 6185–6222.
- Lewis, M.A., and Y. Ben-Zion, 2008, Examination of scaling between earthquake magnitude and proposed early signals in P waveforms from very near source stations in a South African gold mine, *J. Geophys. Res.*, 113(B9), doi:10.1029/2007JB005506.
- Li, Y.-G., and J. E. Vidale, 2001, Healing of the shallow fault zone from 1994–1998 after the 1992 M7.5 Landers, California earthquake, *Geophys. Res. Lett.*, 28(15), 2999–3002.
- Li, Y. G., J. E. Vidale, K. Aki, F. Xu, and T. Burdette, 1998, Evidence of shallow fault zone strengthening after the 1992 M7.5 Landers, California, earthquake, *Science*, 279(5348), 217–219.
- Lin, W., M. Kwasniewski, T. Imamura, and K. Matsuki, 2006, Determination of three-dimensional in-situ stresses from anelastic strain recovery measurement of cores at great depth, *Tectonophysics*, 426, 221–238, doi: 10.1016/j.tecto.2006.02.019.
- Lucier, A., M.D. Zoback, V. Heesackers, Z. Reches and S. Murphy, 2009, Constraining the far-field stress state near a deep South African Gold Mine, *International Journal of Rock Mechanics and Mining Sciences*, 46, 555–567.
- Ma, K.F., J. Mori, S.J. Lee, and S.B. Yu, 2001, Spatial and temporal distribution of slip for the 1999 Chi-Chi, Taiwan earthquake, *Bull. Seism. Soc. Am.*, 91 (5), 1069–1087.
- Ma, K.F., E.E. Brodsky, J. Mori, C. Ji, T.R.A. Song, and H. Kanamori, 2003, Evidence for fault lubrication during the 1999 Chi-Chi, Taiwan, earthquake (Mw7.6), *Geophys. Res. Lett.*, 30(5), 1244, doi:10.1029/2002GL015380.
- Ma, K.F., H. Tanaka, S.R. Song, C.Y. Wang, J.H. Hung, Y.B. Tsai, J. Mori, Y.F. Song, E.C. Yeh, W. Soh, H. Sone, L.W. Kuo, and H.Y. Wu, 2006, Slip zone and energetics of a large earthquake from the Taiwan Chelungpu-fault Drilling Project, *Nature*, 444, 473–476.
- Marsan, D., and I. Lengline, 2008, Extending earthquakes' reach through cascading, *Science*, 319, 1076–1079.
- McGarr, A., M.S. Boettcher, J.B. Fletcher, R. Sell, M.J.S. Johnston, R. Durheim, S. Spottiswoode, and A. Milev, Early results from analyses of broadband records of earthquakes in deep South African gold mines and a brief comparison with results from SAFOD, California, submitted to *Bull. Seism. Soc. Am.*
- Mishima, T., T. Hirono, W. Soh, M. Ikehara, W. Lin, W. Tanikawa, E.C. Yeh, S.R. Song, and C. Wang, 2006, Thermal history estimation of the Taiwan Chelungpu Fault using rock-magnetic methods, *Geophys. Res. Lett.*, 33, L23311, doi:10.1029/2006GL028088.
- Murakami, M., and T. Tagami, 2004, Dating pseudotachylyte of the Nojima fault using the zircon fission-track method, *Geophys. Res. Lett.*, 31 L12604, doi:10.1029/2004GL020211.
- Niu, F.L., P.G. Silver, R.M. Nadeau, and T.V. McEvilly, 2003, Migration of seismic scatterers associated with the 1993 Parkfield aseismic transient event, *Nature*, 426(6966), 544–548.
- Niu, F.L., P.G. Silver, T.M. Daley, X. Cheng and E.L., 2008, Preseismic velocity changes observed from active source monitoring at the Parkfield SAFOD drill site, *Nature*, 454, 204–208.
- Ohtani, T., K. Fujimoto, H. Ito, H. Tanaka, N. Tomida, and T. Higuchi, 2000, Fault rocks and past to recent fluid characteristics from the borehole survey of the Nojima fault ruptured in the 1995 Kobe earthquake, southwest Japan, *Journal of Geophysical Research*, 105 (B7), 16,161–16,171.
- Otsuki, K., T. Uduki, N. Monzawa, and H. Tanaka, 2005, Clayey injection veins and pseudotachylyte from two boreholes penetrating the Chelungpu Fault, Taiwan: Their implications for the contrastive seismic slip behaviors during the 1999 Chi-Chi earthquake, *The Island Arc*, 14, 22–36.
- Rice, J.R., 1992, Fault stress states, pore pressure distributions, and the weakness of the San Andreas Fault, in Evans, B., and Wong, T.-F., eds., *Fault Mechanics and Transport Properties of Rocks*: San Diego, CA, Academic, p. 475–503.
- Rowe, C.D., J.C. Moore, F. Menegheni, and A.W. McKeirnan, 2005, Large-scale pseudotachylytes and fluidized cataclases from an ancient subduction thrust fault, *Geology*, 33, 937–940.
- Scholz, C.H., and F.J. Saucier, 1993, What do the Cajon Pass stress measurements say about stress on the San Andreas fault? Comment on “In situ stress measurements to 3.5 km depth in the Cajon Pass scientific research borehole: Implications for the mechanics of crustal faulting” by Mark D. Zoback and John H. Healy, *J. Geophys. Res.*, 98(B10), 17,867–17,869.
- Sone, H., E.C. Yeh, T. Nakaya, J.H. Hung, K.F. Ma, C.Y. Wang, S.R. Song, and T. Shimamoto, 2007, Mesoscopic structural observations of cores from the Chelungpu fault system, Taiwan Chelungpu-Fault Drilling Project hole-A, Taiwan, *Terrestrial, Atmospheric and Oceanic Sciences*, 18(2), 359–377.
- Sornette, D., and M.J. Werner, 2005, Constraints on the size of the smallest triggering earthquake from the epidemic-type aftershock sequence model, Bath's law, and observed aftershock sequences, *J. Geophys. Res.*, 110, B08304, doi:10.1029/2004JB003535.
- Sulem J., 2007, Stress orientation evaluated from strain localisation analysis in Aigion Fault, *Tectonophysics*, 442(1–4), 3–13.
- Tadokoro, K., 2001, Repeated water injection experiments at the Nojima fault zone, Japan: Induced earthquakes and temporal change in permeability, *ICDP Workshop on Drilling the Chelungpu Fault*, Taiwan, Taipei.
- Tanaka, H., K. Fujimoto, T. Ohtani, and H. Ito, 2001, Structural and chemical characterization of shear zones in the freshly activated Nojima fault, Awaji Island, southwest Japan, *J. Geophys. Res.*, 106 (B5), 8789–8810.

- Tanaka, H., W.M.Chen, C.Y. Wang, K.F. Ma, N. Urata, J. Mori, and M. Anod, 2006, Frictional heat from faulting of the 1999 Chi-Chi, Taiwan, earthquake, *Geophys. Res. Lett.*, 33, L16316, doi:10.1029/2006GL026673.
- Tanaka, H., K. Omura, T. Matsuda, R. Ikeda, K. Kobayashi, M. Murakami, and K. Shimada, 2007, Architectural evolution of the Nojima fault and identification of the activated slip layer by Kobe earthquake, *J. Geophys. Res.*, 112, B07304, doi:10.1029/2005JB003977.
- Tanikawa, W., and T. Shimamoto, 2009, Frictional and transport properties of the Chelungpu fault from shallow borehole data and their correlation with seismic behavior during the 1999 Chi-Chi earthquake, *J. Geophys. Res.*, 114, B01402, doi:10.1029/2008JB005750.
- Tenthorey, E., S.F. Cox, and H.F. Todd, 2003, Evolution of strength recovery and permeability during fluid-rock reaction in experimental fault zones, *Earth and Planetary Science Letters*, 206(1-2), 161–172.
- Tsukahara, H., R. Ikeda, and K. Yamamoto, 2001, In situ stress measurements in a borehole close to the Nojima Fault, *Island Arc*, 10, 261–265.
- UNDP (UN Development Programme), Bureau for Crisis Prevention and Recovery, 2004, *Reducing Disaster Risk: A Challenge For Development A Global Report*. New York: J.S. Swift, Co.
- Vidale, J. E., and Y.-G. Li, 2003, Damage to the shallow Landers fault from the nearby Hector Mine earthquake, *Nature*, 421, 524–526.
- Williams, C.F., F.V. Grubb, and S.P. Galanis Jr., 2004, Heat flow in the SAFOD pilot hole and implications for the strength of the San Andreas Fault, *Geophys. Res. Lett.*, 31, L15S14, doi:10.1029/2003GL019352.
- Working Group on California Earthquake Probabilities, 2008, *The Uniform California Earthquake Rupture Forecast, Version 2 (UCERF 2)*, U.S. Geological Survey Open-File Report 2007-1437 and California Geological Survey Special Report 203 [<http://pubs.usgs.gov/of/2007/1437/>].
- Wu, H.-Y., K.-F. Ma, M. Zoback, N. Boness, H. Ito, J.-H. Hung, and S. Hickman, 2007, Stress orientations of Taiwan Chelungpu-Fault Project (TCDP) hole-A as observed from geophysical logs *Geophys. Res. Lett.*, doi:10.1029/2006GL028050.
- Yamamoto, K., and Y. Yabe, 2001, Stresses at sites close to the Nojima Fault measured from core samples, *The Island Arc*, 10, 266–281.
- Yeh, E.C., H. Sone, T. Nakaya, K.H. Ian, S.R. Song, J.H. Hung, W. Lin, T. Hirono, C.Y. Wang, K.F. Ma, W. Soh, and M. Kinoshita, 2007, Core description and characteristics of fault zones from Hole-A of the Taiwan Chelungpu-Fault Drilling Project, *Terrestrial, Atmospheric and Oceanic Sciences*, 18 (2), 327–357.
- Yasuhara, H., C. Marone, and D. Elsworth, 2005, Fault zone restrengthening and frictional healing: The role of pressure solution, *J. Geophys. Res.*, 110, B06310, doi:10.1029/2004JB0033272005.
- Zoback, M.D., and J.H. Healy, 1992, In situ stress measurements to 3.5 km depth in the Cajon Pass scientific research borehole: Implications for the mechanics of crustal faulting, *J. Geophys. Res.*, 97(B4), 5039–5057.
- Zoback, M.D., S. Hickman, and W.E. Ellsworth, 2007, The role of fault zone drilling, in *Treatise on Geophysics*, edited by G. Schubert, pp. 649-674, Elsevier.
- Zoback, M.D., and S.H. Hickman, 2005, Preliminary observations of stress and fluid pressure in and near the San Andreas Fault at depth in the SAFOD boreholes, *Eos Trans. AGU*, 86(52), Fall Meet. Suppl., Abstract T21A-0438.
- Zoback, M.D., C.A. Barton, M. Brudy, D.A. Castillo, T. Finkbeiner, B.R. Grollimund, D.B. Moos, P. Peska, C.D. Ward, and D.J. Wiprut, 2003, Determination of stress orientation and magnitude in deep wells, *Int. J. Rock Mech. Min. Sci.*, 40, 1049–1076.





The Rapid Drilling workshop and the accompanying report were supported by the Southern California Earthquake Center, the International Continental Scientific Drilling Program, the University of California, Santa Cruz, and the University of Kyoto.

